Interconversion between multicomponent slider-on-deck and palladium capsule: Regulation of catalysis and encapsulation

Isa Valiyev, Indrajit Paul, Yi-Fan Li, Emad Elramadi, and Michael Schmittel*

Center of Micro and Nanochemistry and (Bio)Technology, Organische Chemie I, School of Science and Technology, University of Siegen, Adolf-Reichwein-Str. 2, D-57068 Siegen, Germany

E-mail: schmittel@chemie.uni-siegen.de

Table of Contents

1. Synthesis

1.1 General information.

All reagents were obtained from commercial suppliers and used without further purification. Technical grade solvents were distilled prior to use. ^{1}H-, ^{13}C-, ^{1}H-^{1}H-COSY-, ^{1}H-^{1}H-NOESY-, and ^{1}H-DOSY NMR spectra were recorded at 298 K using the deuterated solvent as the lock. The chemical shifts refer to the residual protiated fraction of the solvent ($CHDCl_2$: δ_H = 5.32 ppm, δ_C = 53.8 ppm; CHD_2CN: δ_H = 1.94 ppm, δ_C = 1.32, 118.3 ppm). Abbreviations were used in ^{1}H NMR assignments to describe splitting patterns (s: singlet, d: doublet, t: triplet, dd: doublet of doublets, ddd: doublet of doublets of doublets, brs: broad singlet, dt: doublet of triplets, m: multiplet), the value of coupling constant(s) is reported in Hertz (Hz) and the number of protons is implied. The numbering of carbon atoms is usually not in accordance with IUPAC nomenclature guidelines. Melting points were measured on a Büchi SMP-20 and are uncorrected. Infrared spectra were recorded using a Perkin Elmer Spectrum-Two FT-IR spectrometer. Fluorescence spectra were measured on a Cary Eclipse Fluorescence Spectrophotometer. UV-vis spectra were measured on a Cary Win 50. Binding constants were determined through UV-vis titrations in combination with a 1:1 binding formula of two ligands or with SPECFIT/32TM global analysis system by Spectrum Software Associates (Marlborough, MA). Electrospray ionization mass spectra (ESI-MS) were recorded on a Thermo-Quest LCQ Deca instrument and the theoretical isotopic distributions of the mass signals were calculated using molecular weight calculator software (https://omics.pnl.gov/software/molecular-weight-calculator). Elemental analysis was performed using the EA-3000 CHNS analyzer. Column chromatography was performed on silica gel 60 (60−230 mesh). Thin Layer Chromatography (TLC) was performed using Merck silica gel (60 F254) sheets. Compounds **3** and **G** were obtained commercially. Compounds **2**,[1] **4**,[2] **5**,[2] and **6**[3] were synthesized according to known procedures. The spectral data of this compound was in good agreement with those in the literature reports.

1.2 Ligands

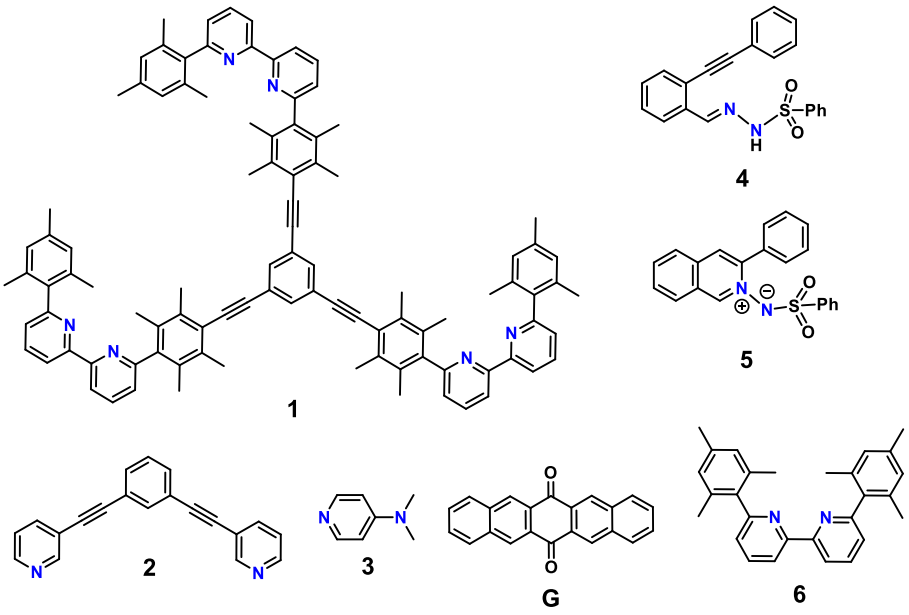

Chart 1. Structure of ligands.

1.3 Synthesis and characterization of ligands

Synthesis and characterization of ligand **1**

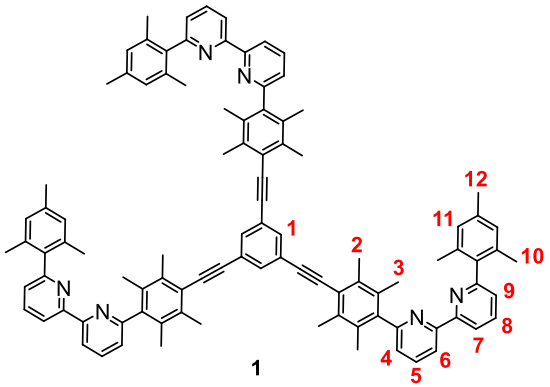

In a 100-mL sealed tube, a solution of 1,3,5-tribromobenzene (100 mg, 318 μmol) and 6-(4-ethynyl-2,3,5,6-tetramethyl)phenyl-6'-(2,4,6-trimethyl)phenyl-2,2'-bipyridine[4] (548 mg, 1.27 mmol) in dry THF (25.0 mL) and dry *N*,*N*-diisopropylamine (20.0 mL) was degassed by using two freeze-

pump-thaw cycles. Then, $Pd(PPh_3)_4$ (34.6 mg, 30.0 µmol) was added under N_2 atmosphere. One additional freeze-pump-thaw cycle was used for degassing. The mixture was stirred at 85 °C for 12 h. After evaporation of the solvent, the crude product was extracted with CH_2Cl_2 (200 mL), washed by water (100 mL × 3) and dried over anhydrous Na_2SO_4. Further purification was achieved by column chromatography on silica gel using 20% CH_2Cl_2 in *n*-hexane furnishing the product as a colorless solid (377 mg, 277 µmol, 87%). R_f = 0.15 (SiO_2, 20% CH_2Cl_2 in *n*-hexane) **MP:** > 250 °C. **IR** (KBr): 3571, 3242, 3172, 3124, 3011, 1768, 1752, 1682, 1639, 1588, 1189, 1036, 954, 871, 858 cm^{-1}. **^{1}H NMR (CD_2Cl_2, 500 MHz):** δ 2.01 (s, 18H, 2-H), 2.09 (s, 18H, 10-H), 2.36 (s, 9H, 12-H), 2.62 (s, 18H, 3-H), 6.99 (s, 6H, 11-H), 7.23 (dd, ^3J = 7.8 Hz, ^4J = 1.3 Hz, 3H, 4-H), 7.24 (dd, ^3J = 7.8 Hz, ^4J = 1.3 Hz, 3H, 9-H), 7.80 (s, 3H, 1-H), 7.85 (t, ^3J = 7.8 Hz, 3H, 5-H), 7.88 (t, ^3J = 7.8 Hz, 3H, 8-H), 8.37 (dd, ^3J = 7.8 Hz, ^4J = 1.3 Hz, 3H, 6-H), 8.42 (dd, ^3J = 7.8 Hz, ^4J = 1.3 Hz, 3H, 7-H) ppm. **^{13}C NMR (CD_2Cl_2, 125 MHz):** δ 17.7, 18.7, 20.4, 21.2, 90.3, 95.9, 119.2, 119.4, 122.9, 125.0, 125.1, 125.3, 128.6, 132.3, 133.6, 136.1, 136.8, 137.3, 137.5, 137.8, 138.4, 142.1, 156.3, 156.5, 159.5, 160.4 ppm. **ESI-MS**: *m/z* (%) = 682.8 (100) $[1•(2H)]^{2+}$, 1364.8 (60) $[1•H]^+$**. Elemental analysis:** Calcd. for $C_{99}H_{90}N_6•H_2O$: C, 86.05; H, 6.71; N, 6.08. Found: C, 86.00; H, 6.99; N, 5.77.

Characterization of literature-known ligand **2**[1]

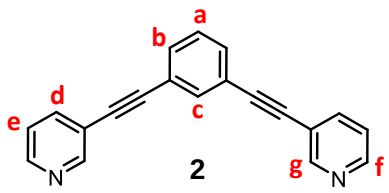

2

^{1}H NMR (CD_2Cl_2, 500 MHz): 7.31 (ddd, ^3J = 7.0 Hz, ^3J = 7.1 Hz, ^5J = 1.1 Hz, 2H, e-H), 7.41 (td, ^3J = 7.8 Hz, ^5J = 1.0 Hz, 1H, a-H), 7.56 (dd, ^3J = 7.8 Hz, ^4J = 1.8 Hz, 2H, b-H), 7.75 (t, ^4J = 1.8 Hz, 1H, c-H), 7. 84 (dt, ^3J = 7.0 Hz, ^4J = 2.1 Hz, 2H, d-H), 8.55 (dd, ^3J = 7.1 Hz, ^4J = 2.1 Hz, 2H, f-H), 8.76 (s, 2H, g-H) ppm.

1.4 Synthesis and characterization of complexes

Synthesis of complex $[Cu_3(\mathbf{1})]^{3+}$

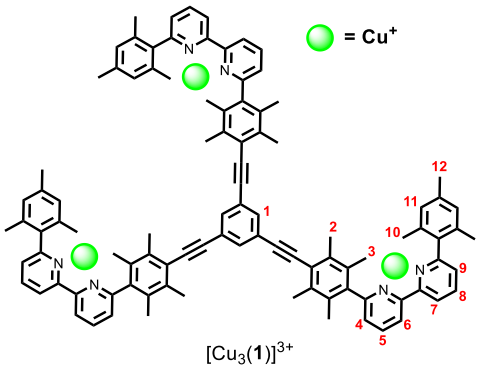

Into an NMR tube, ligand **1** (900 µg, 659 nmol) was dissolved in 500 µL of CD_2Cl_2, then $[Cu(CH_3CN)_4]PF_6$ (738 µg, 1.97 µmol) was added, and subsequently the NMR was recorded. **Yield**: Quantitative. **MP:** > 250 °C. **IR** (KBr): 3571, 3242, 3172, 3124, 3011, 1768, 1752, 1682, 1639, 1588, 1189, 1036, 993, 954, 871, 858, 831, 713, 679, 618, 589 cm^{-1}. **^{1}H NMR (CD_2Cl_2, 500 MHz):** δ 1.94 (s, 18H, 2-H), 2.00 (s, 18H, 10-H), 2.32 (s, 9H, 12-H), 2.56 (s, 18H, 3-H), 6.97 (s, 6H, 11-H), 7.63 (t, ^3J = 7.5 Hz, 6H, 5-, 8-H), 7.73 (s, 3H, 1-H), 8.23 (dd, ^3J = 7.5 Hz, ^4J = 1.4 Hz, 3H, 9/4-H), 8.24 (dd, ^3J = 7.5 Hz, ^4J = 1.4 Hz, 3H, 4/9-H), 8.29 (d, ^3J = 7.5 Hz, 3H, 7/6-H), 8.30 (d, ^3J = 7.5 Hz, 3H, 6/7-H) ppm. **ESI-MS**: *m/z* (%) = 518.2 (50) $[Cu_3(\mathbf{1})]^{3+}$, 849.8 (100) $[Cu_3(\mathbf{1}) + PF_6]^{2+}$. **Elemental analysis:** Calcd. for $C_{99}H_{90}Cu_3F_{18}N_6P_3$: C, 59.77; H, 4.56; N, 4.22. Found: C, 59.59; H, 4.67; N, 4.53.

Synthesis of slider-on-deck $[Cu_3(\mathbf{1})(\mathbf{2})]^{3+}$

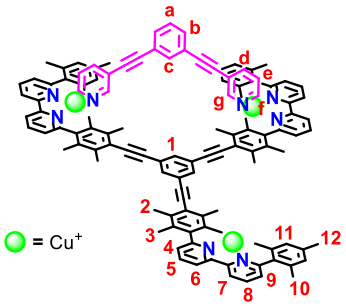

In an NMR tube, deck **1** (900 µg, 659 nmol) was dissolved in the mixture of 400 µL of CD_2Cl_2 and 100 µL of CD_3CN. Then, $[Cu(CH_3CN)_4]PF_6$ (738 µg, 1.97 µmol) and biped **2** (185 µg, 659 nmol) were added. Subsequently, the NMR was recorded. **Yield**: Quantitative. **MP:** > 250 °C. **^{1}H NMR (CD_2Cl_2 : CD_3CN (4:1), 500 MHz):** δ 1.92 (s, 18H, 2-H), 2.23 (s, 18H, 10-H), 2.47 (s, 18H, 3-H), 2.98 (s, 9H, 12-H), 6.46 (dd, ^3J = 9.1 Hz, ^4J = 1.2 Hz, 2H, f-H), 6.83 (s, 6H, 11-H), 7.08 (t, ^3J = 9.8 Hz, 1H, a-H), 7.17 (dd, ^3J = 9.1 Hz, ^3J = 9.2 Hz, 2H, e-H), 7.41 (d, ^3J = 9.8 Hz, 2H, b-H), 7.48 (d, ^3J = 8.8 Hz, 3H, 9/4-H), 7.52 (d, ^3J = 8.8 Hz, 3H, 4/9-H), 7.55 (s, 3H, 1-H), 7.68 (s, 1H, c-H), 7.71 (brs, 2H, g-H), 7.83 (dd, ^3J = 9.2 Hz, ^4J = 1.2 Hz, 2H, d-H), 8.14 (dd, ^3J = 9.0 Hz, ^3J = 8.8 Hz, 3H, 8/5-H), 8.16 (dd, ^3J = 9.0 Hz, ^3J = 8.8 Hz, 3H, 5/8-H), 8.30 (d, ^3J = 9.0 Hz, 3H, 7/6-H), 8.33 (d, ^3J = 9.0 Hz, 3H, 6/7-H) ppm. **ESI-MS: ESI-MS**: *m/z* (%) = 611.4 (60) $[Cu_3(\mathbf{1})(\mathbf{2})]^{3+}$, 989.4 (100) $[Cu_3(\mathbf{1})(\mathbf{2}) + PF_6]^{2+}$**. Elemental analysis:** Calcd. for $C_{119}H_{102}Cu_3F_{18}N_8P_3 \bullet H_2O$: C, 62.48; H, 4.58; N, 4.90. Found: C, 62.42; H, 4.20; N, 5.09.

Synthesis of literature-known complex[1] $[Pd_2(\mathbf{2})]^{4+}$

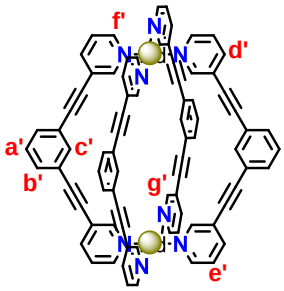

C = $[Pd_2(\mathbf{2})_4]^{4+}$

= Pd^{2+}

Ligand **2** (185 µg, 659 nmol) was dissolved in an NMR tube in a mixture of 400 µL of CD_2Cl_2 and 100 µL of CD_3CN. Then $[Pd(CH_3CN)_4](BF_4)_2$ (146 µg, 329 nmol) was added, and subsequently the NMR was recorded. **^{1}H NMR (CD_2Cl_2 : CD_3CN (4:1), 500 MHz):** 7.42 (t, ^3J = 8.0 Hz, 4H, a'-H), 7.56-7.61 (m, 16H, b'-, e'-H), 8.00 (dd, ^3J = 8.0 Hz, ^4J = 1.5 Hz, 8H, d'-H), 8.03 (brs, 4H, c'-H), 9.34 (d, ^3J = 5.6 Hz, 8H, f'-H), 9.50 (s, 8H, g'-H) ppm.

Synthesis of complex $[Pd_2(\mathbf{2})_4\mathbf{G}]^{4+}$ + **G** (**G@C** + **G**)

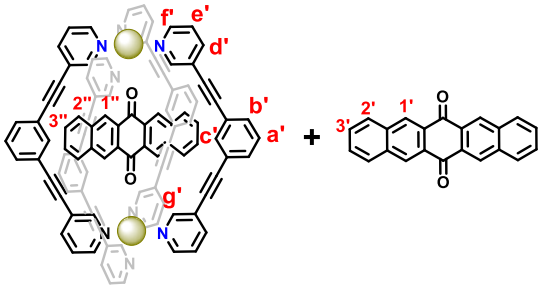

Ligand **2** (185 µg, 659 nmol) was dissolved in an NMR tube in the mixture of 400 µL of CD_2Cl_2 and 100 µL of CD_3CN. Into the NMR tube $[Pd(CH_3CN)_4](BF_4)_2$ (146 µg, 329 nmol) was added. After formation of cage (**C**), pentacene-6,13-dione (**G**) (76.1 µg, 247 nmol) was added and subsequently the NMR was recorded. **^{1}H NMR (CD_2Cl_2 : CD_3CN (4:1), 500 MHz):** 5.49 (brs, 4H, c'-H), 7.04 (dd, ^3J = 6.4 Hz, ^4J = 3.1 Hz, 4H, 3"-H), 7.14 (t, ^3J = 9.0 Hz, 4H, a'-H), 7.28 (dd, ^3J = 9.0 Hz, ^4J = 1.1 Hz, 8H, b'-H), 7.72 (dd, ^3J = 6.3 Hz, ^4J = 3.2 Hz, 2H, 3'-H), 7.76 (dd, ^3J = 8.1 Hz, ^3J = 7.9 Hz, 8H, e'-H), 7.92 (dd, ^3J = 6.4 Hz, ^4J = 3.1 Hz, 4H, 2"-H), 8.10 (dt, ^3J = 7.9 Hz, ^4J = 1.7 Hz, 8H, d'-H), 8.16 (dd, ^3J = 6.3 Hz, ^4J = 3.2 Hz, 2H, 2'-H), 8.91 (s, 2H, 1'-H), 9.42 (dd, ^3J = 8.1 Hz, ^4J = 1.8 Hz, 8H, f'-H), 9.66 (s, 8H, g'-H), 10.06 (s, 4H, 1"-H) ppm. **ESI-MS**: *m/z* (%) = 411.0 (25) $[Pd_2(\mathbf{2})_4\mathbf{G}]^{4+}$, 576.1 (55) $[Pd_2(\mathbf{2})_4\mathbf{G} + BF_4]^{3+}$, 908.0 (100) $[Pd_2(\mathbf{2})_4\mathbf{G} + 2(BF_4)]^{2+}$**.**

2. NMR Spectra: ^{1}H, ^{13}C, ^{1}H-^{1}H COSY

2.1 NMR spectra of ligands: ^{1}H, ^{13}C, ^{1}H-^{1}H COSY

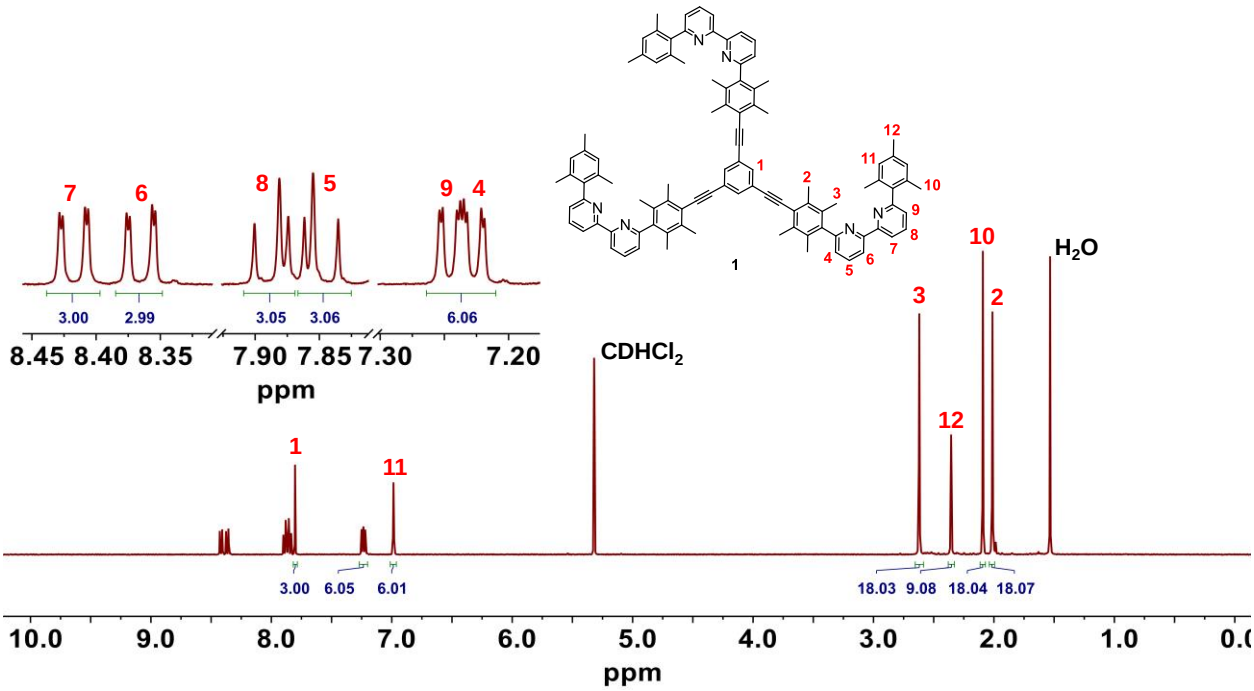

Figure S1. ^{1}H NMR spectrum (CD_2Cl_2, 500 MHz, 298 K) of ligand **1**.

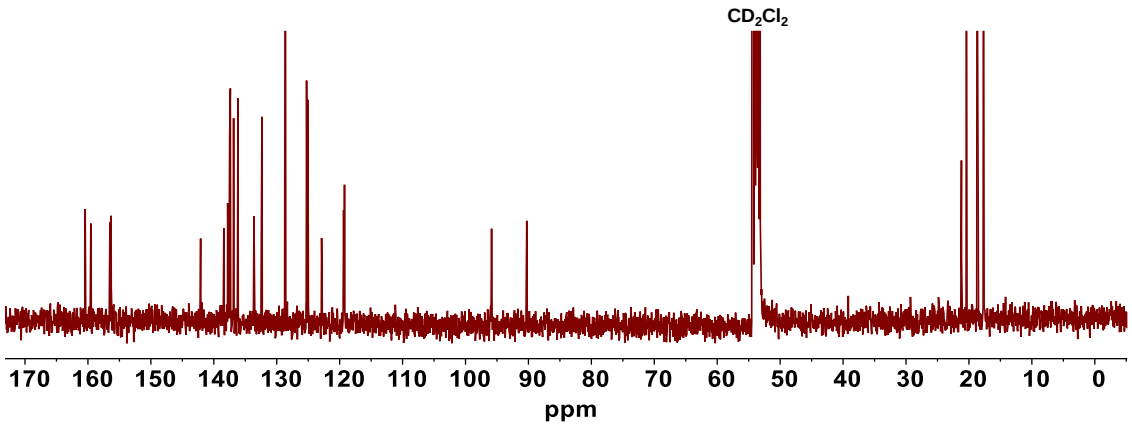

Figure S2. ^{13}C NMR spectrum (CD_2Cl_2, 125 MHz, 298 K) of ligand **1**.

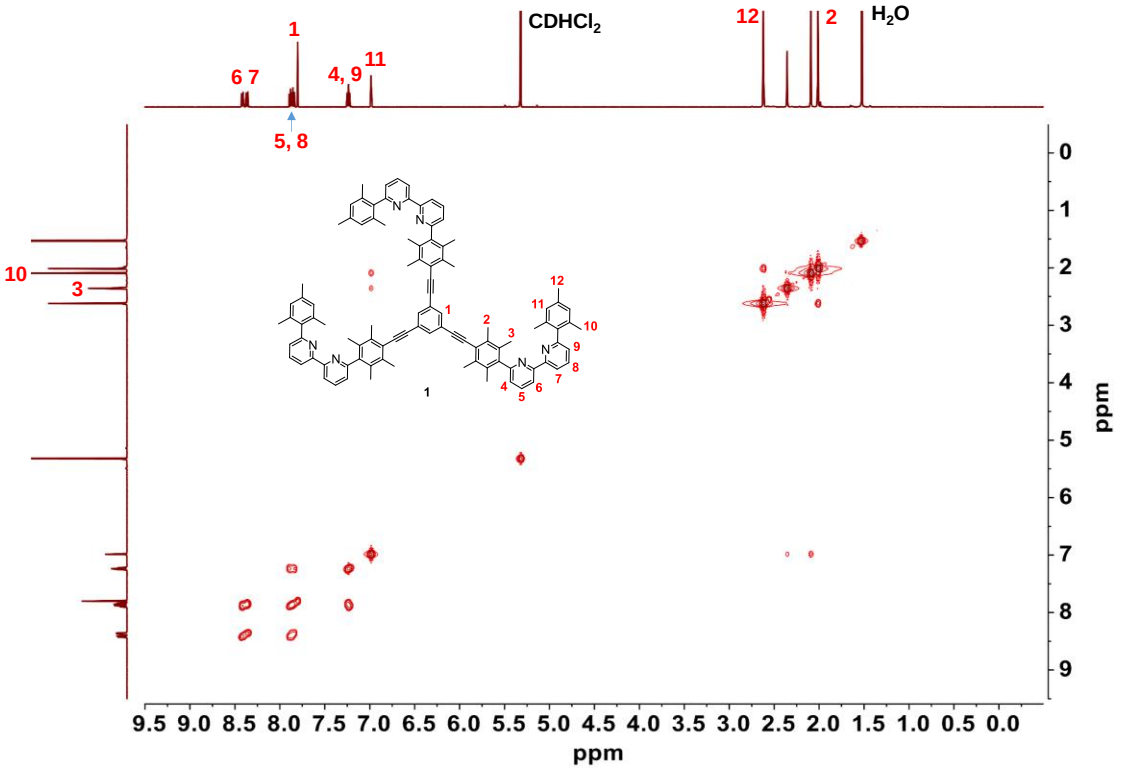

Figure S3. ^{1}H-^{1}H COSY NMR spectrum (CD_2Cl_2, 500 MHz, 298 K) of ligand **1**.

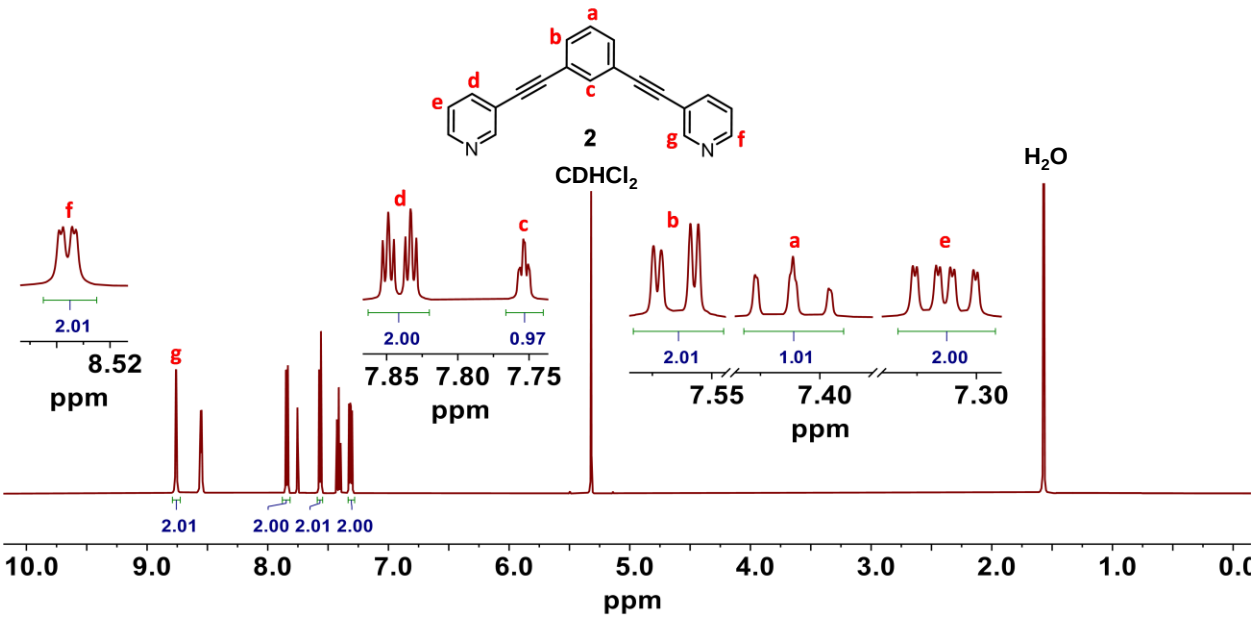

Figure S4. ^{1}H NMR spectrum (CD_2Cl_2, 500 MHz, 298 K) of ligand **2**.

2.2 NMR spectra of complexes: ^{1}H, ^{13}C, ^{1}H-^{1}H COSY

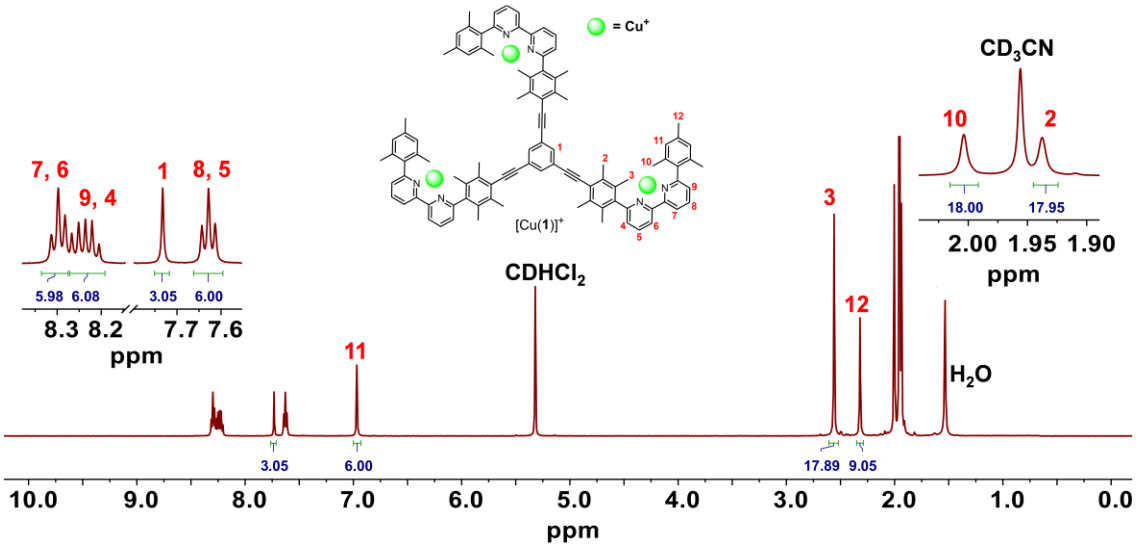

Figure S5. ^{1}H NMR spectrum (CD_2Cl_2, 500 MHz, 298 K) of complex $[Cu_3(\mathbf{1})]^{3+}$.

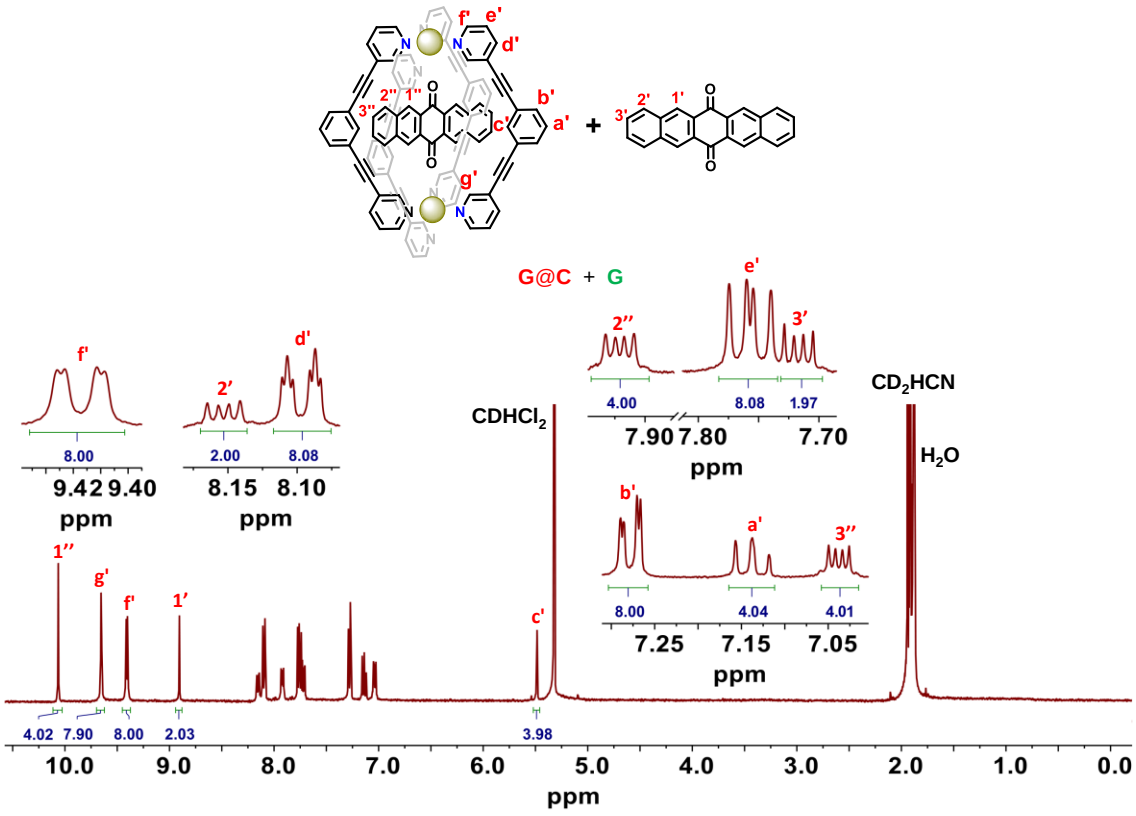

Figure S6. ^{1}H NMR spectrum (CD_2Cl_2:CD_3CN = 4:1, 500 MHz, 298 K) of complex **G@C** + **G**.

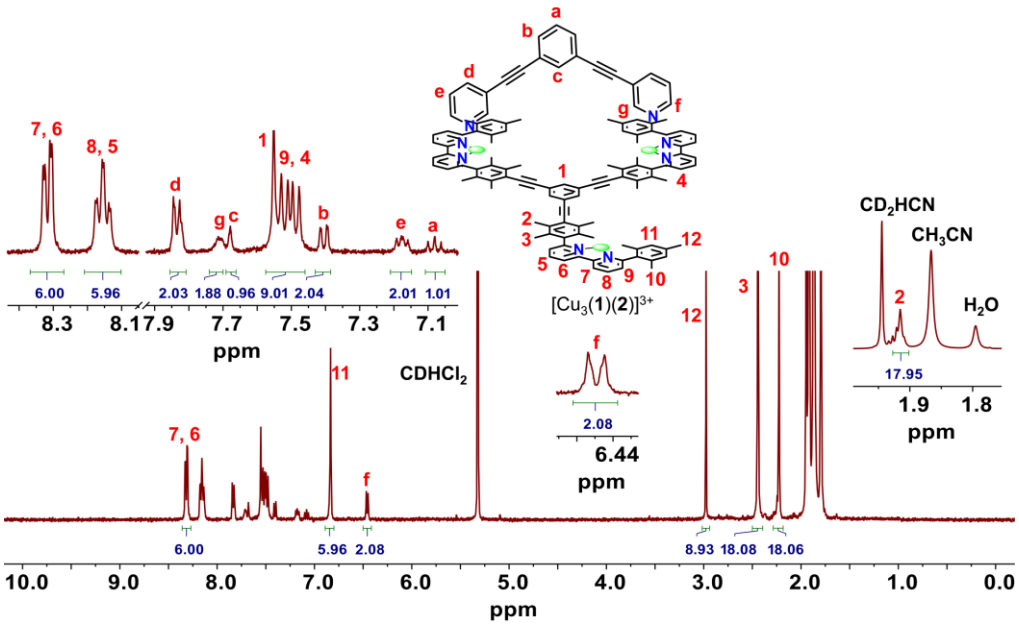

Figure S7. ^{1}H NMR spectrum (CD_2Cl_2:CD_3CN = 4:1, 500 MHz, 298 K) of complex $[Cu_3(\mathbf{1})(\mathbf{2})]^{3+}$.

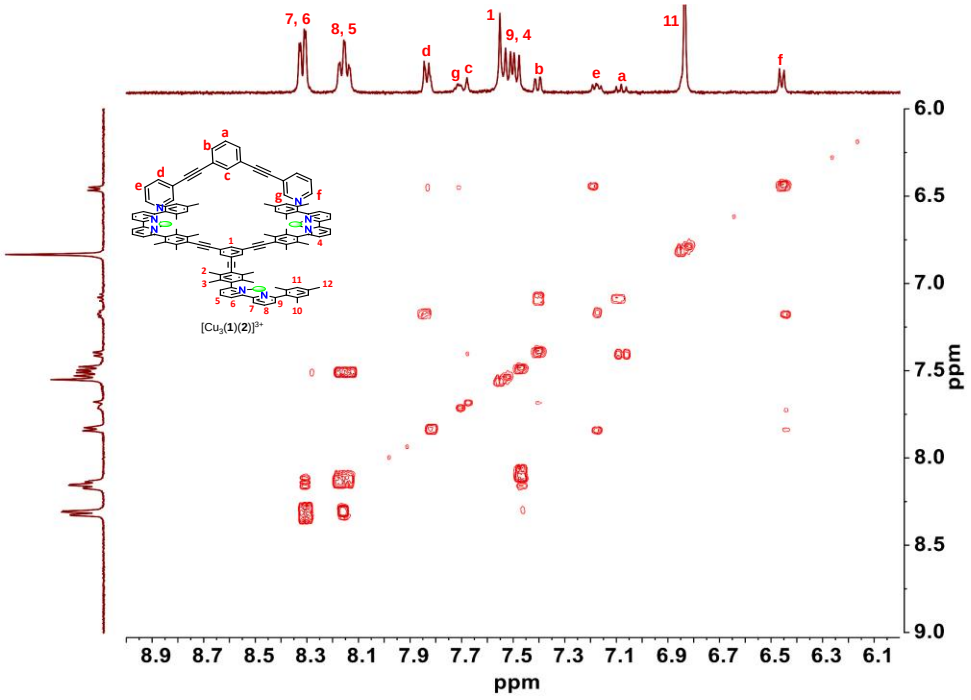

Figure S8. Partial ^{1}H-^{1}H COSY NMR spectrum (CD_2Cl_2:CD_3CN = 4:1, 500 MHz, 298 K) of complex $[Cu_3(\mathbf{1})(\mathbf{2})]^{3+}$.

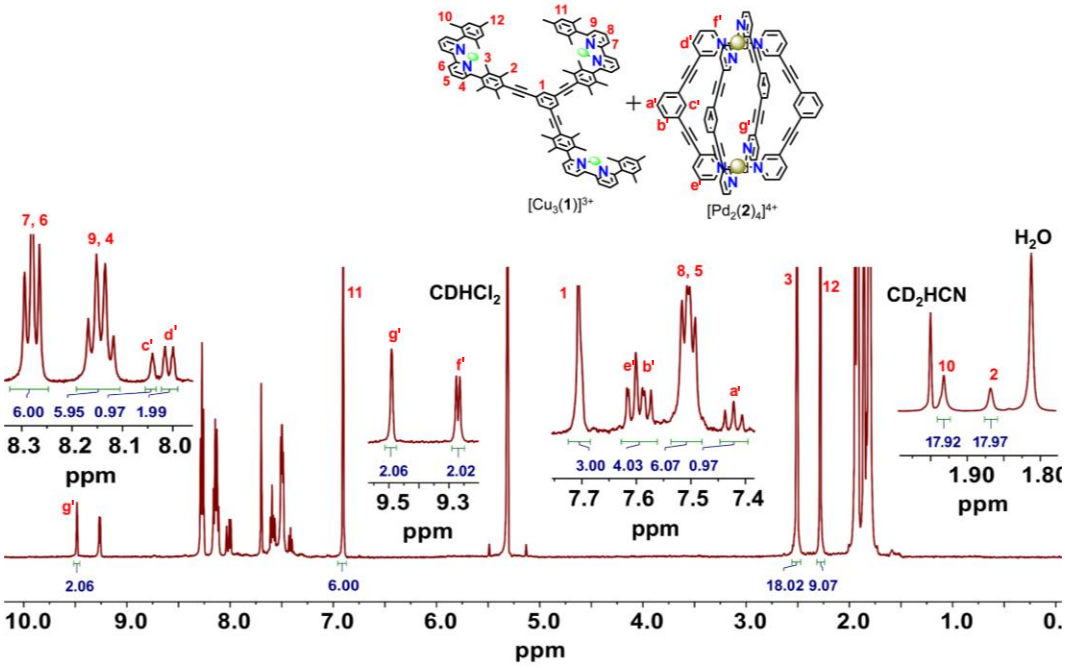

Figure S9. ^{1}H NMR spectrum (CD_2Cl_2:CD_3CN = 4:1, 500 MHz, 298 K) of complex $[Cu_3(\mathbf{1})]^{3+}$ + $[Pd_2(\mathbf{2})_4]^{4+}$.

2.3 ^{1}H NMR spectra of Networked States

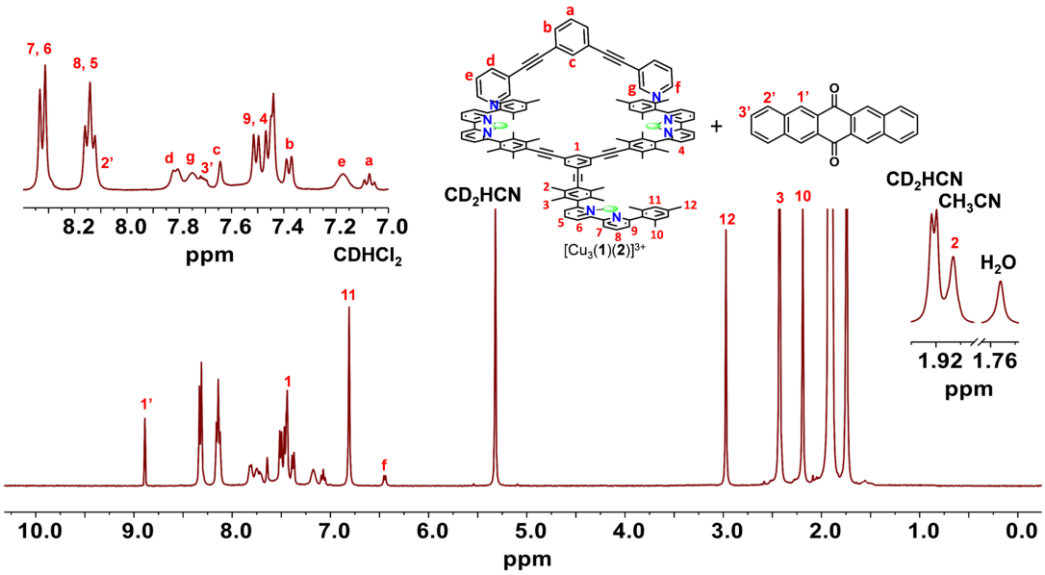

Figure S10. ^{1}H NMR spectrum (CD_2Cl_2:CD_3CN = 4:1, 500 MHz, 298 K) of complex $[Cu_3(\mathbf{1})(\mathbf{2})]^{3+}$ + **G**.

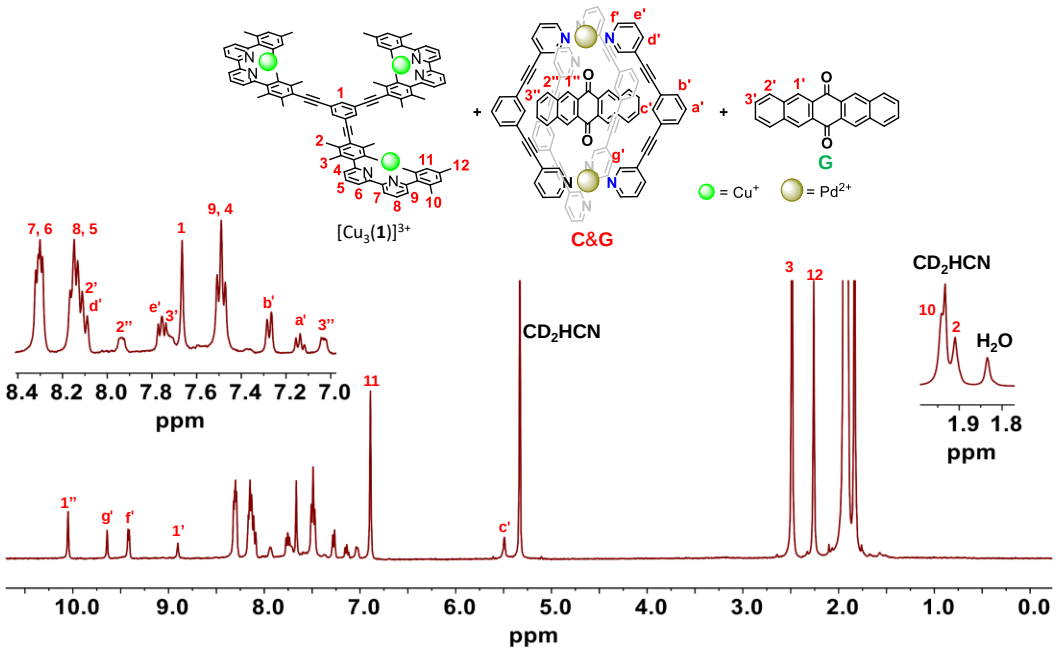

Figure S11. ^{1}H NMR spectrum (CD_2Cl_2:CD_3CN = 4:1, 500 MHz, 298 K) of complex $[Cu_3(\mathbf{1})]^{3+}$ + $[Pd_2(\mathbf{2})_4\mathbf{G}]^{4+}$ + **G**.

2.4 ^{1}H NMR spectra showing reversibility of Networked States

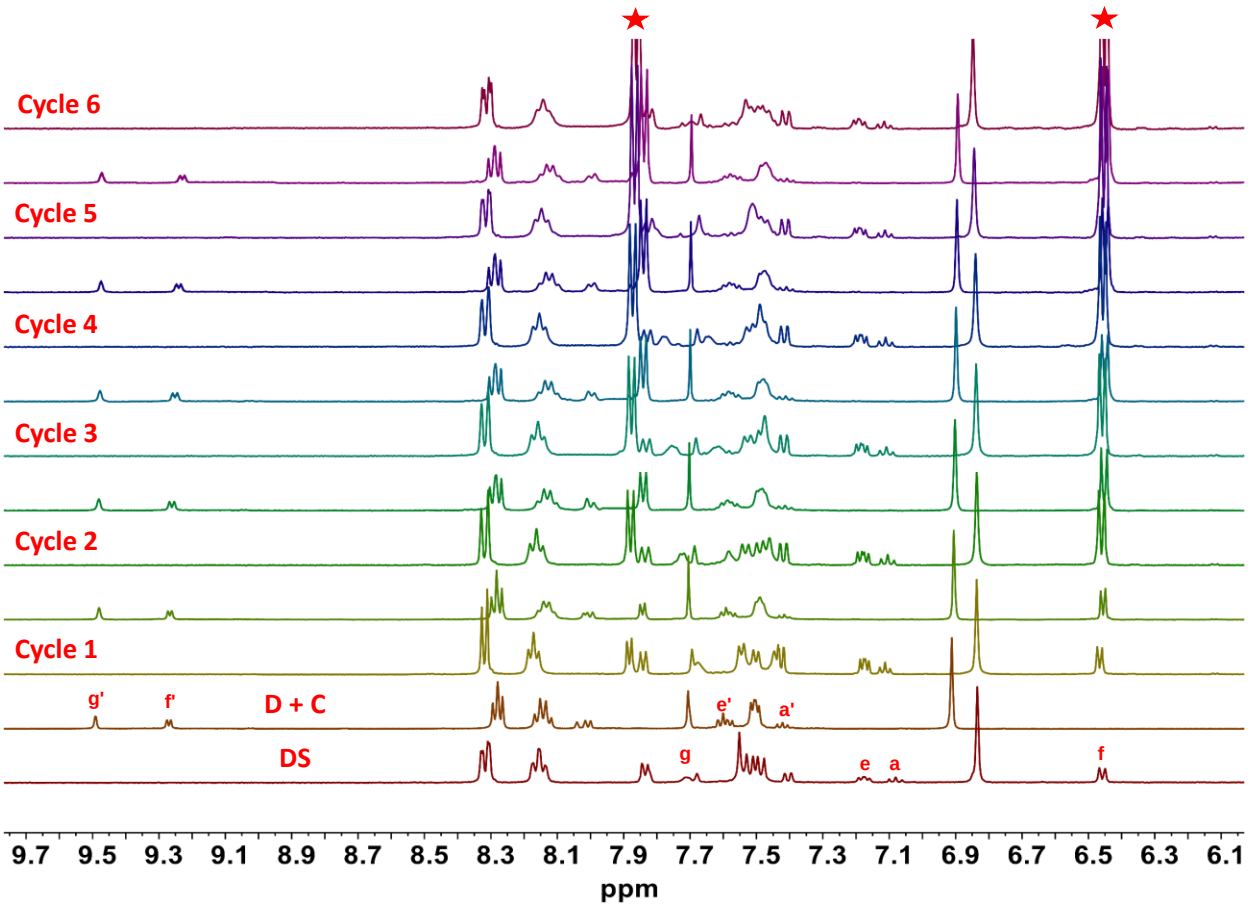

Figure S12. Reversibility of the networked system in presence of Pd^{2+} and DMAP over six cycles monitored by ^{1}H NMR (400 MHz). The red star indicates NMR peaks of $[Pd(DMAP)_4]^{2+}$. Starting from the first cycle, NMR peaks of $[Pd(DMAP)_4]^{2+}$ appear in the system.

2.5 ^{1}H-^{1}H NOESY NMR spectra of G@C

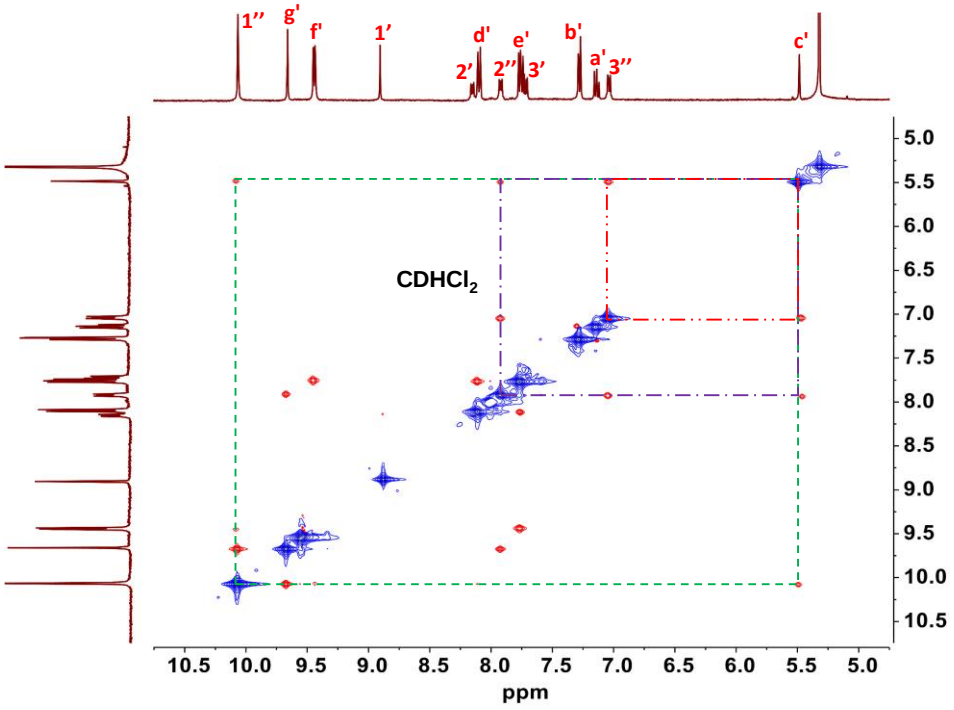

Figure S13. ^{1}H-^{1}H NOESY NMR spectrum of encapsulation of pentacenedione in cage (**G@C**) in CD_2Cl_2 : CD_3CN = 4:1 (600 MHz, 298 K).

3. DOSY NMR Spectra

Calculation of hydrodynamic radius from DOSY

The diffusion coefficient D for slider-on-deck and guest encapsulated cage (**G@C**) were obtained from the DOSY spectrum. The corresponding hydrodynamic radius was calculated by using the Stokes-Einstein equation:

$$r = kBT/6\pi\eta D$$

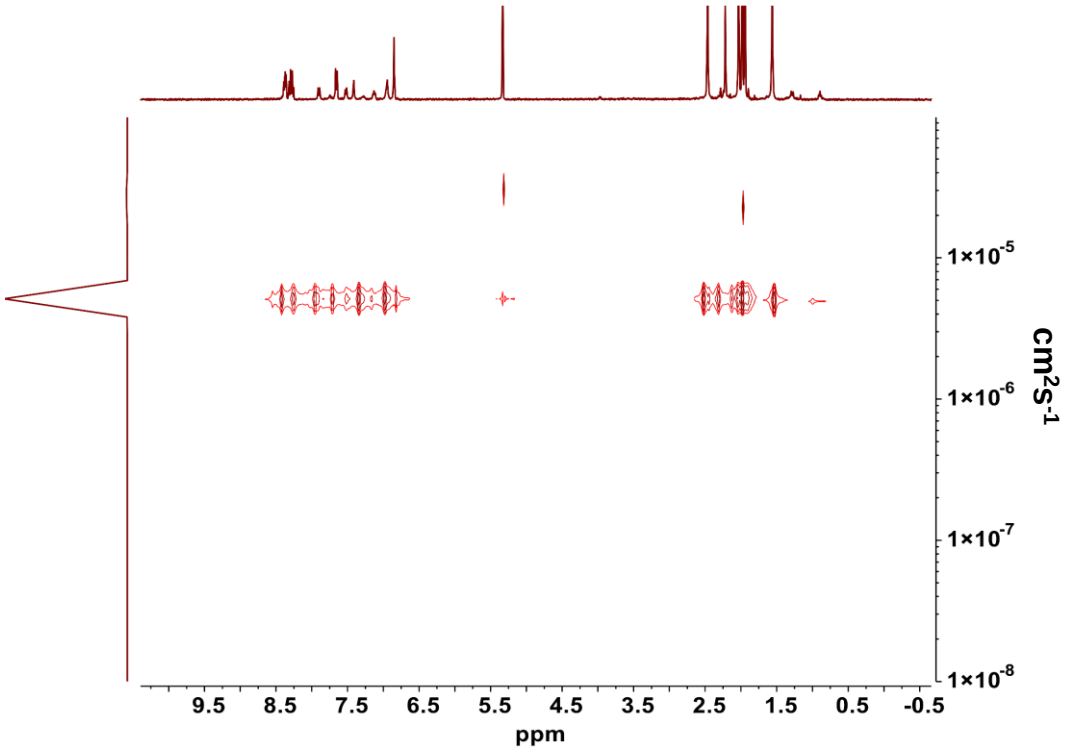

Figure S14. ^{1}H-DOSY NMR of slider-on-deck in CD_2Cl_2:CD_3CN = 4:1 (600 MHz, 298 K). Diffusion coefficient D = 5.69 × 10^{-10} m^2s^{-1}, hydrodynamic radius r = 9.28 Å.

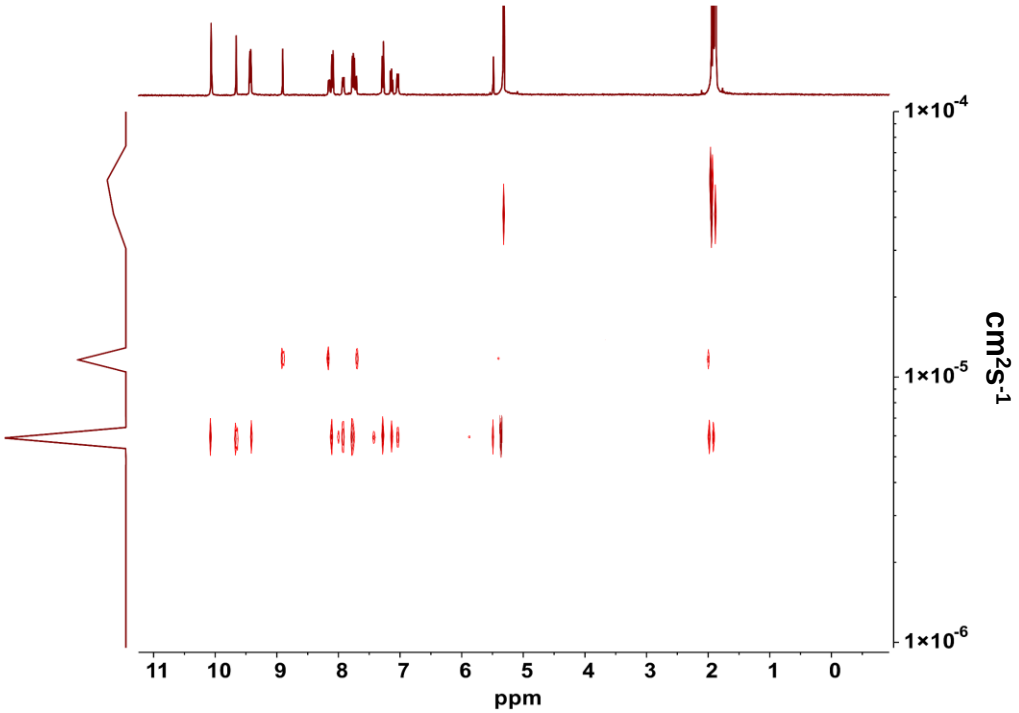

Figure S15. ^{1}H-DOSY NMR of guest encapsulated cage (**G@C**) in CD_2Cl_2:CD_3CN = 4:1 (600 MHz, 298 K). Diffusion coefficient for **G@C** D = 6.24 × 10^{-10} m^2s^{-1}, hydrodynamic radius r = 8.47 Å. ^{1}H-DOSY NMR spectrum shows two sets of signals for **G@C** (long) and free **G** (short).

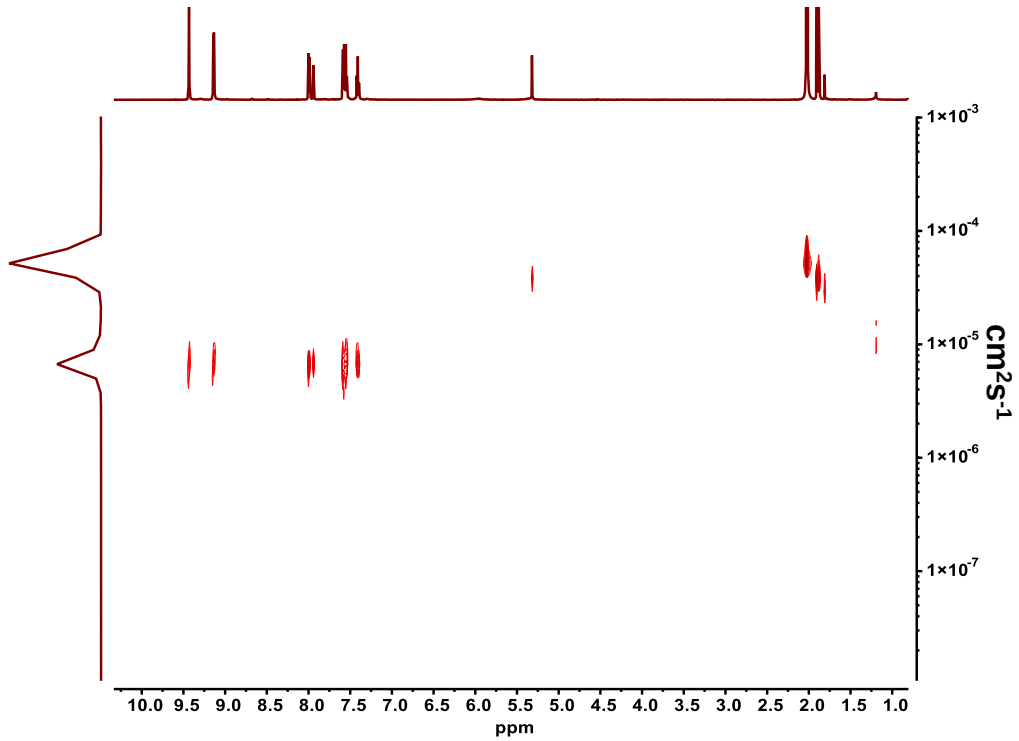

Figure S16. ^{1}H-DOSY NMR of cage (**C**) in CD_2Cl_2:CD_3CN = 4:1 (600 MHz, 298 K). Diffusion coefficient D = 6.38 × 10^{-10} m^2s^{-1}, hydrodynamic radius r = 8.27 Å.

4. Variable Temperature ^{1}H NMR Spectra

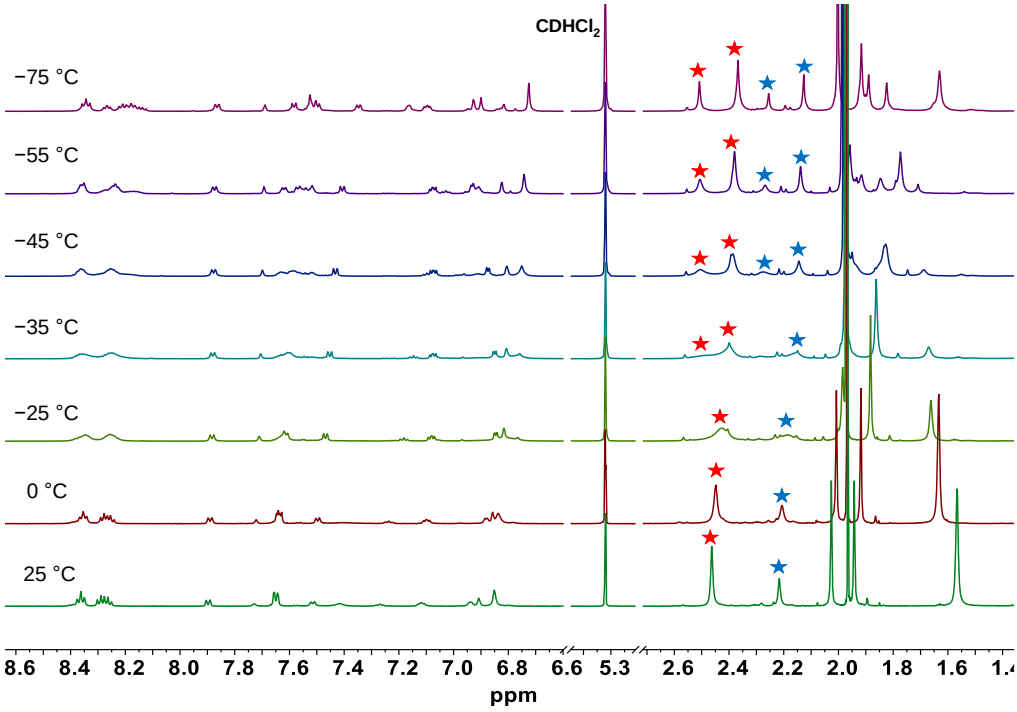

Figure S17. Partial ^{1}H VT-NMR (CD_2Cl_2, 600 MHz) of slider-on-deck showing the splitting of proton 3-H (red asterisk marked) and 12-H (blue asterisk marked).

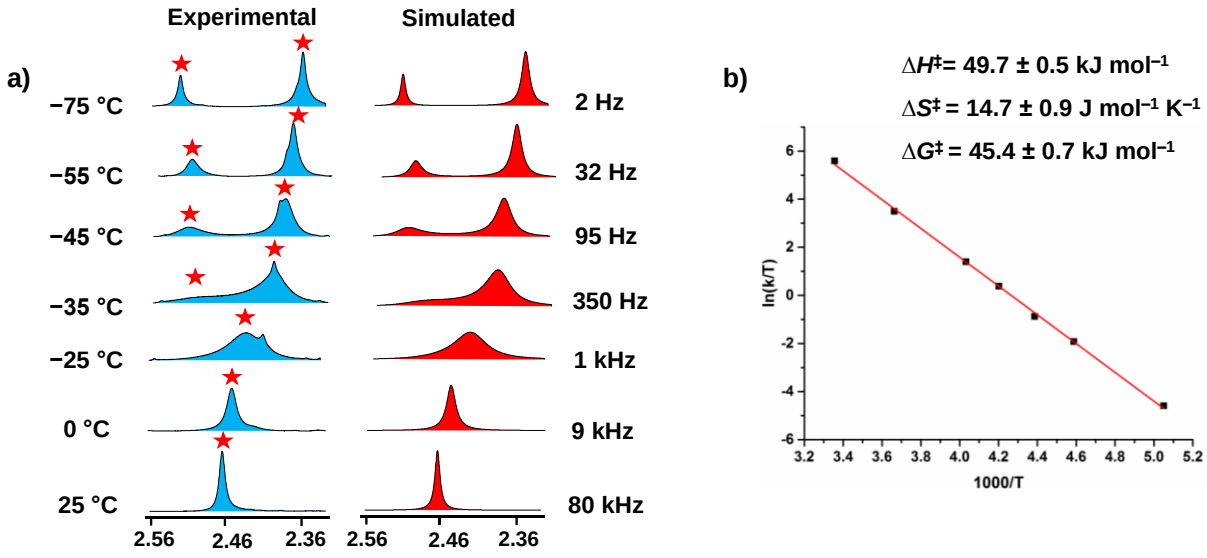

Figure S18. (a) Experimental and simulated ^{1}H VT-NMR (CD_2Cl_2, 600 MHz) of slider-on-deck shows the splitting of 3-H (red asterisk marked) and (b) Eyring plot for rotational exchange in slider-on-deck.

5. Catalytic Experiments

5.1 Catalytic cycles of the aza Hopf cyclization

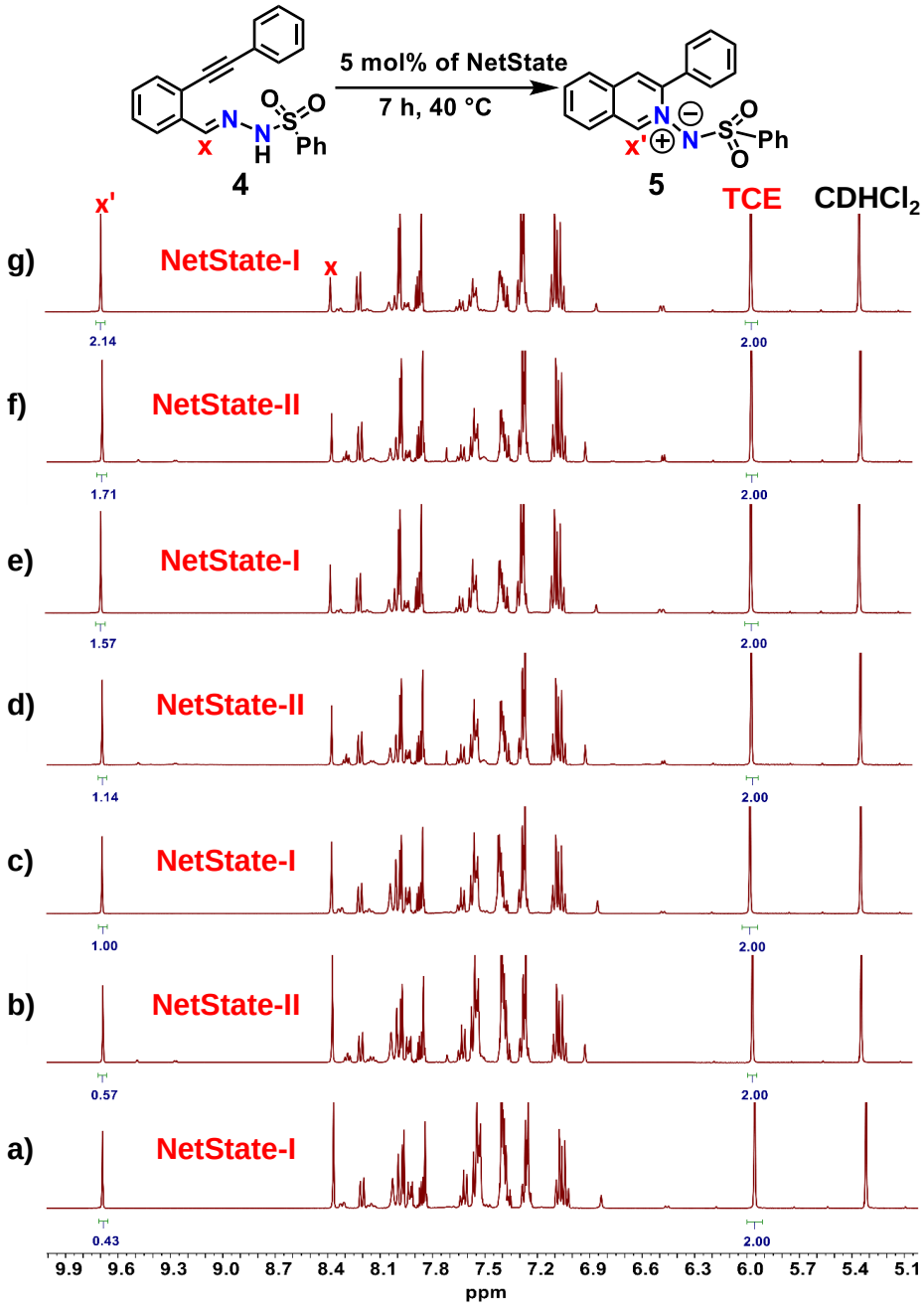

Figure S19. Catalytic cycles of the cyclization to the isoquinolinium imide **5** in presence of 5 mol% of the NetState-I/II. ^{1}H NMR (400 MHz, CD_2Cl_2:CD_3CN = 4:1, 298 K) spectrum obtained after (a) heating the reaction mixture at 40 °C for 7 h in presence of $[Cu_3(\mathbf{1})(\mathbf{2})]^{3+}$ in an NMR tube revealed that the cyclized product **5** (singlet at δ = 9.69 ppm) was formed (yield = 43% with respect to internal standard TCE). (b)

After addition of 0.5 equiv of $[Pd(CH_3CN)_4](BF_4)_2$ with respect to ligand **2**, followed by subsequent heating at 40 °C for 7 h. The reaction yielded product **5** in 14% (derived from total yield 57% = 43% + 14%). (c) After addition of 2 equiv of DMAP with respect to ligand **2**. Reaction under the same conditions yielded 43% (100% = 57% + 43%). (d) After addition of 0.5 equiv of $[Pd(CH_3CN)_4](BF_4)_2$ with respect to ligand **2**. Using the same conditions, the reaction yielded 14% of **5** (114% = 100% + 14%). (e) After addition of 2 equiv of DMAP with respect to ligand **2.** Using the same conditions, the reaction yielded 43% of **5** (total yield 157% = 114% + 43%). (f) After addition of 0.5 equiv of $[Pd(CH_3CN)_4](BF_4)_2$ with respect to ligand **2**, at identical conditions, the reaction yielded 14% of **5** (total yield 171% = 157% + 14%). (g) After addition of 2 equiv of DMAP with respect to ligand **2**. Using the same conditions, the reaction yielded 43% of **5** (214% = 171% + 43%).

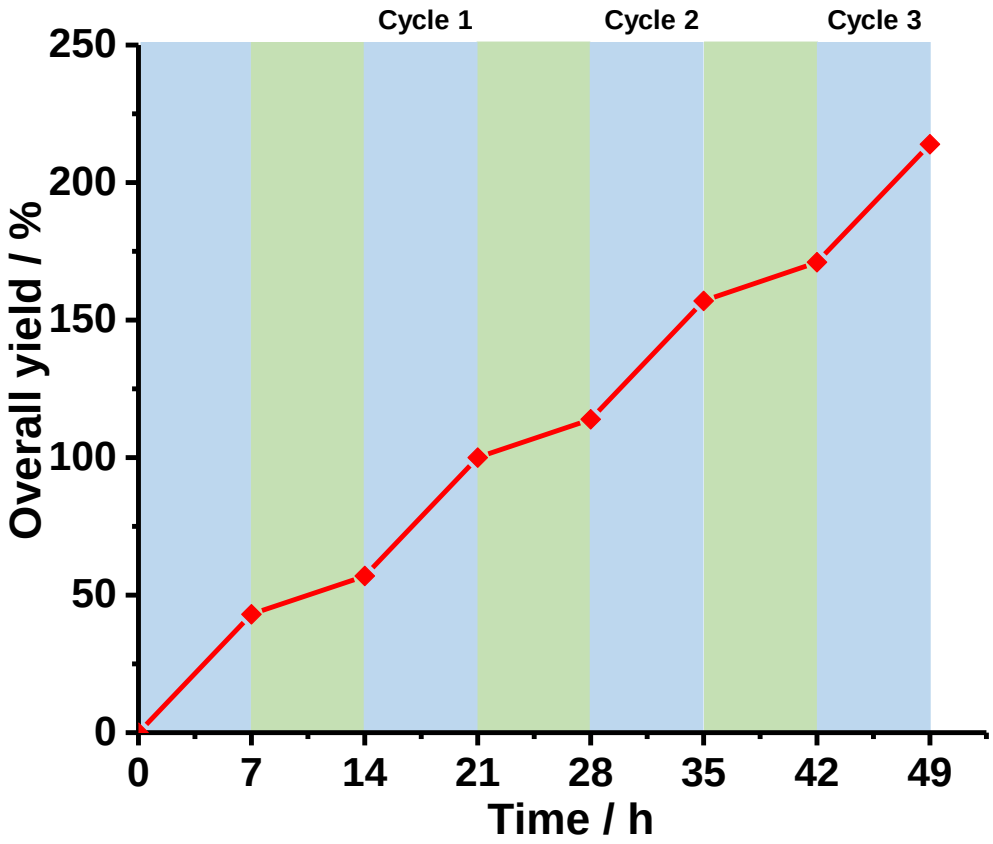

Figure S20. The graphical representation of the catalytic cycles of the aza Hopf cyclization in presence of 5 mol% of the system.

5.2 Control experiments of catalysis

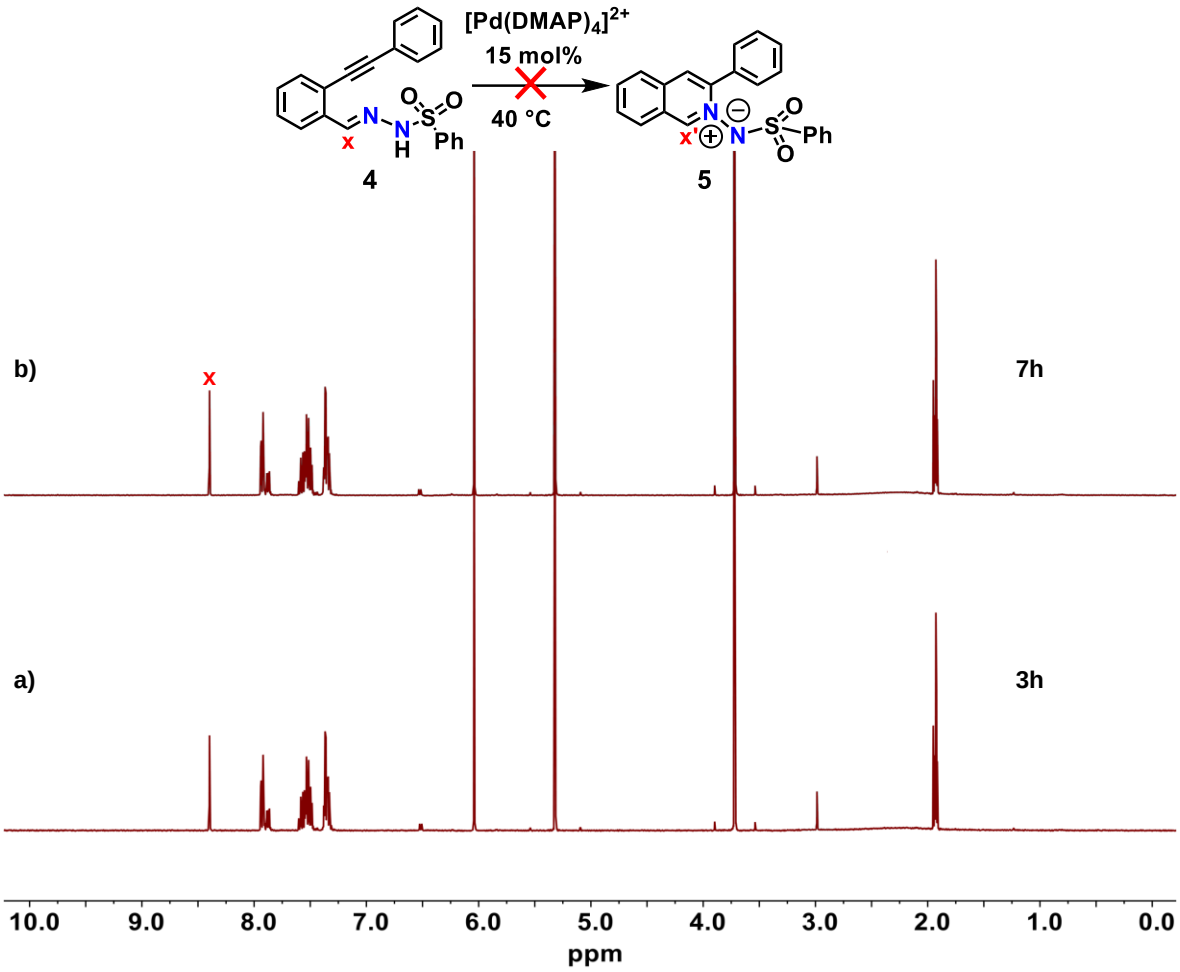

Figure S21. ^{1}H NMR spectra (CD_2Cl_2:CD_3CN = 4:1, 400 MHz, 298 K) of the attempt to cyclize **4** in presence of $[Pd(DMAP)_4]^{2+}$ (15 mol%) at 40 °C for a) 3 h and b) 7 h. No product was obtained.

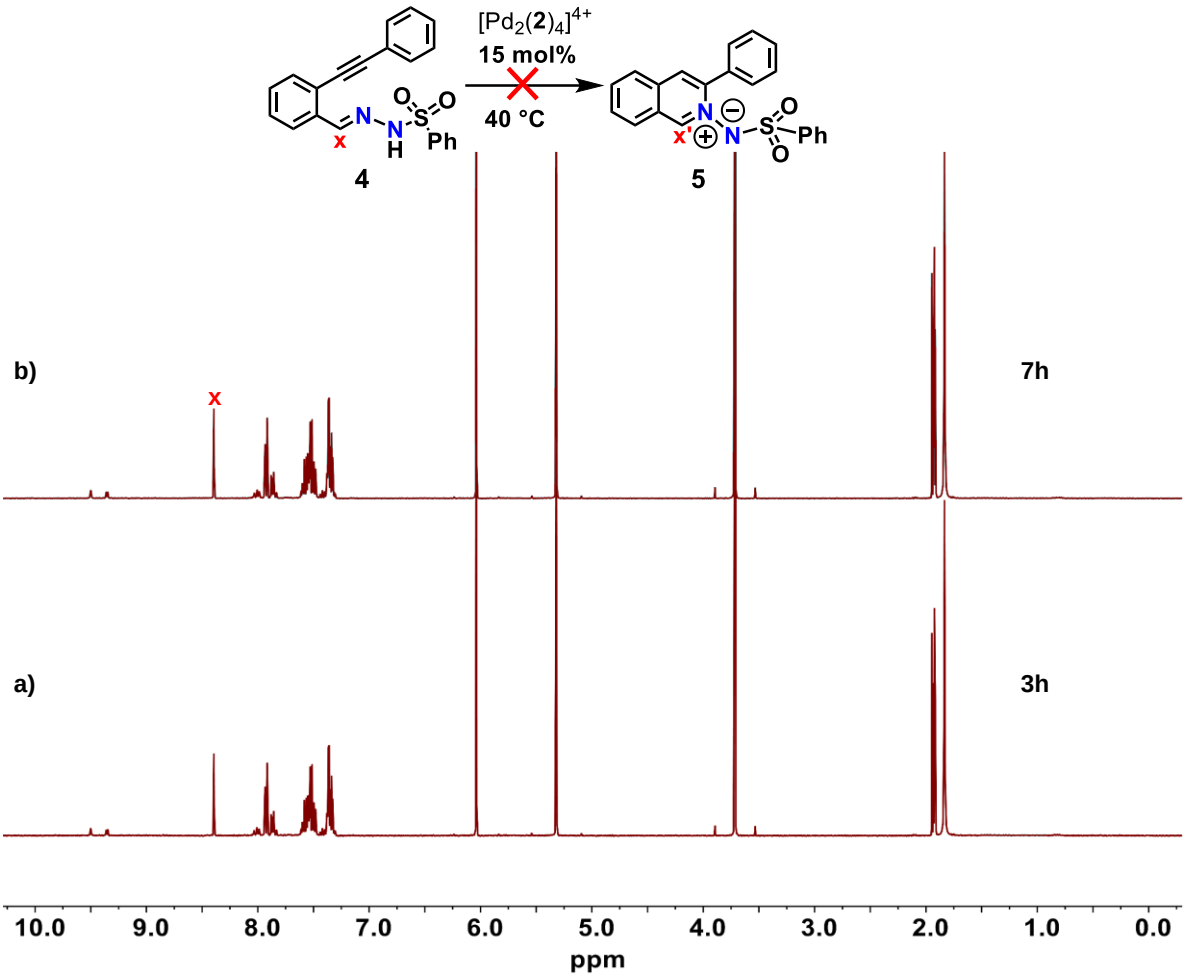

Figure S22. ^{1}H NMR spectra (CD_2Cl_2:CD_3CN = 4:1, 400 MHz, 298 K) of the attempt to cyclize **4** in presence of cage ($[Pd_2(\mathbf{2})_4]^{4+}$) (15 mol%) at 40 °C for a) 3 h and b) 7 h. No product was obtained.

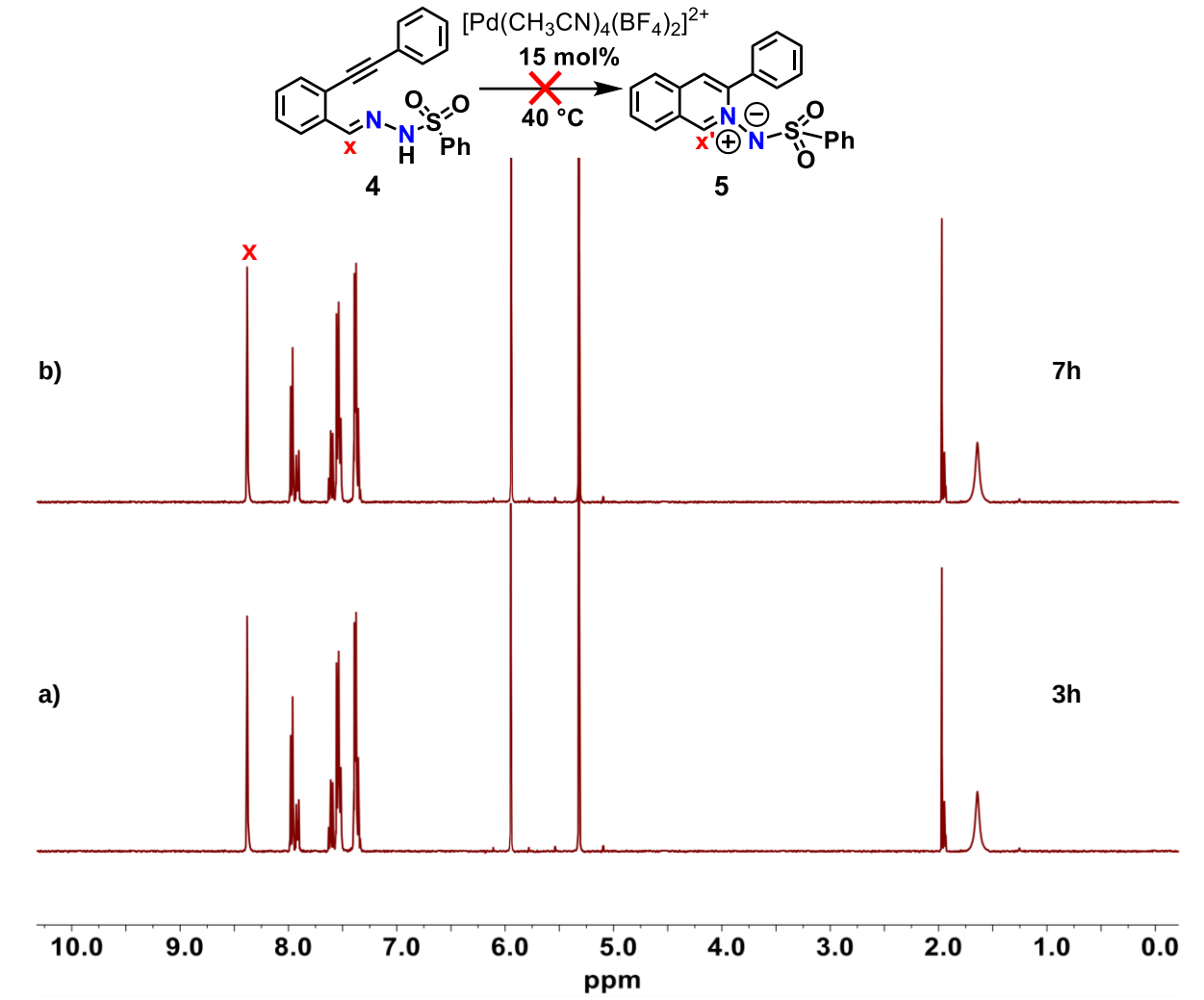

Figure S23. ^{1}H NMR spectra (CD_2Cl_2:CD_3CN = 4:1, 400 MHz, 298 K) of the attempt to cyclize **4** in presence of $[Pd(CH_3CN)_2(BF_4)_2]^{2+}$ (15 mol%) at 40 °C for a) 3 h and b) 7 h. No product was obtained.

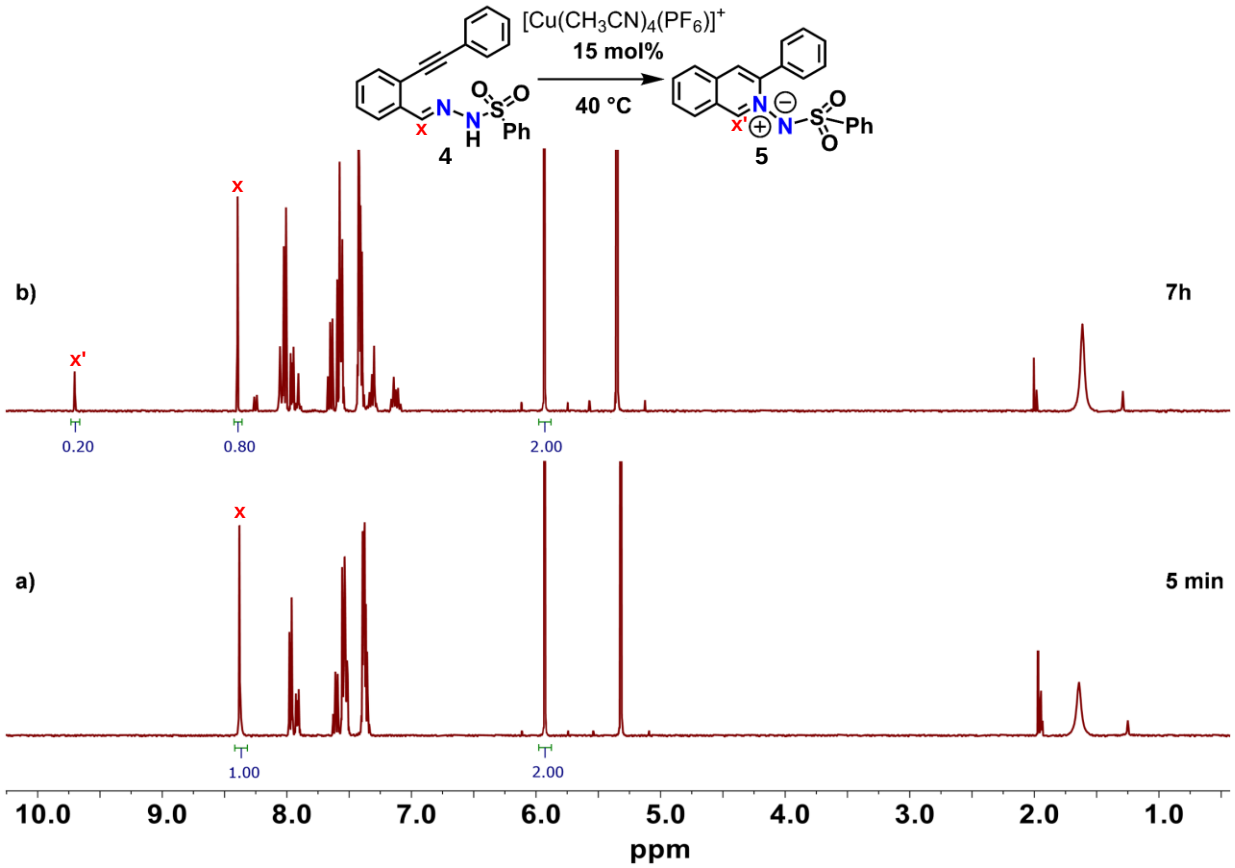

Figure S24. ^{1}H NMR spectra (CD_2Cl_2:CD_3CN = 4:1, 400 MHz, 298 K) of the cyclization of **4** in presence of $[Cu(CH_3CN)_4](PF_6)$ (15 mol%) at a) 25 °C for 5 min and b) 40 °C for 7 h. It revealed that the cyclized product **5** (singlet at δ 9.69 ppm) was formed (yield = 20%; calculated with respect to internal standard TCE).

6. ESI-MS Spectra

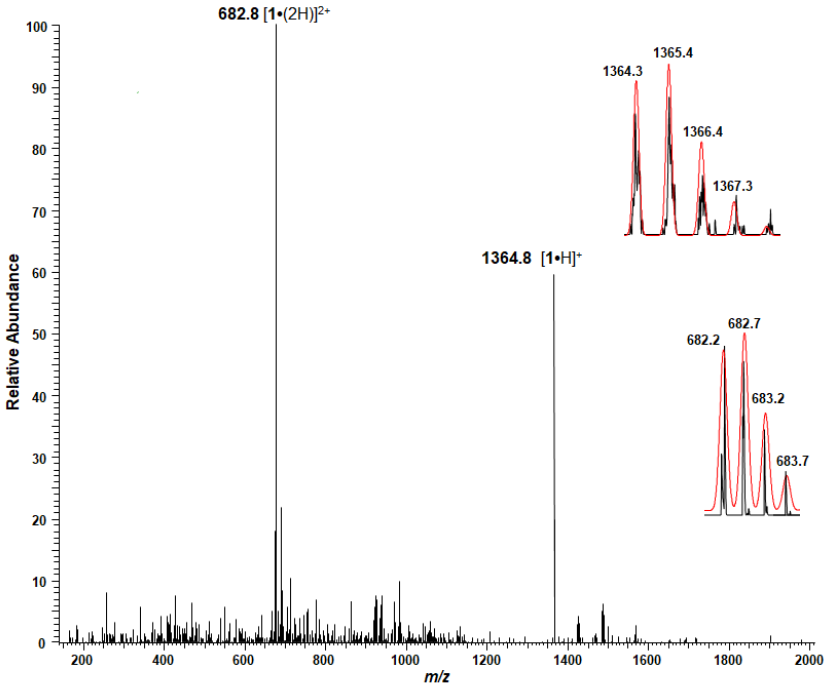

Figure S25. ESI-MS spectrum of **1**•H^+ in DCM. Red traces represent the simulated hyperfine splitting.

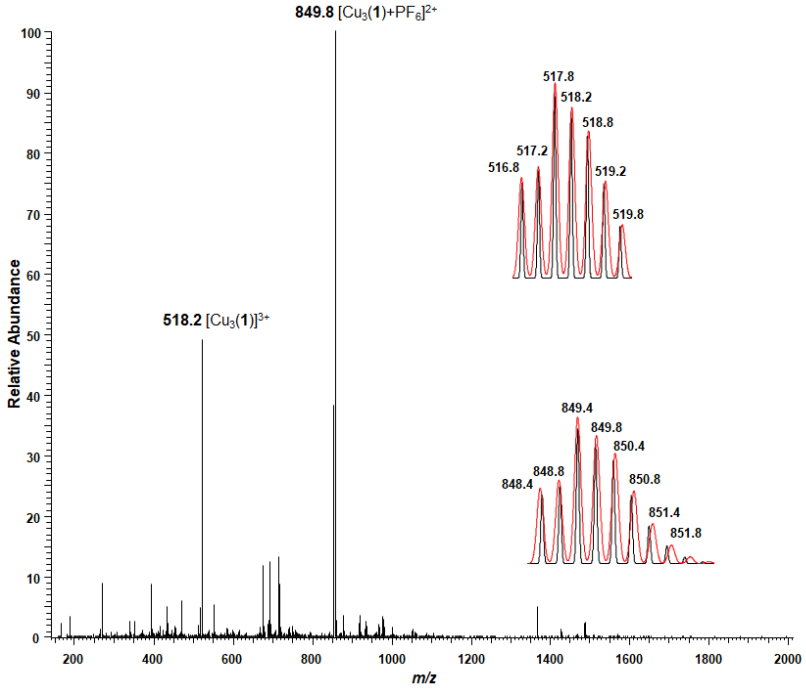

Figure S26. ESI-MS spectrum of $[Cu_3(\mathbf{1})]^{3+}$ in DCM. Red traces represent the simulated hyperfine splitting.

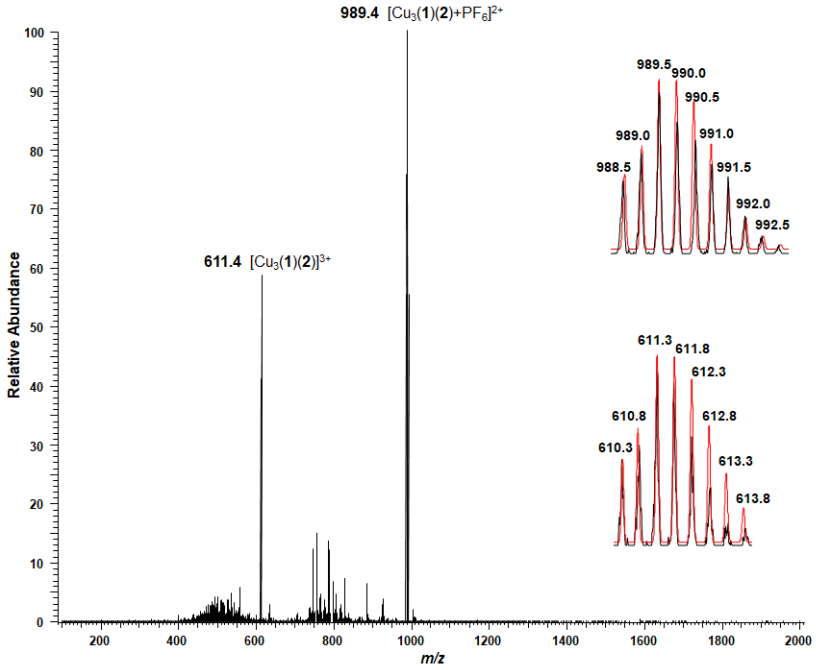

Figure S27. ESI-MS spectrum of $[Cu_3(\mathbf{1})(\mathbf{2})]^{3+}$ in DCM. Red traces represent the simulated hyperfine splitting.

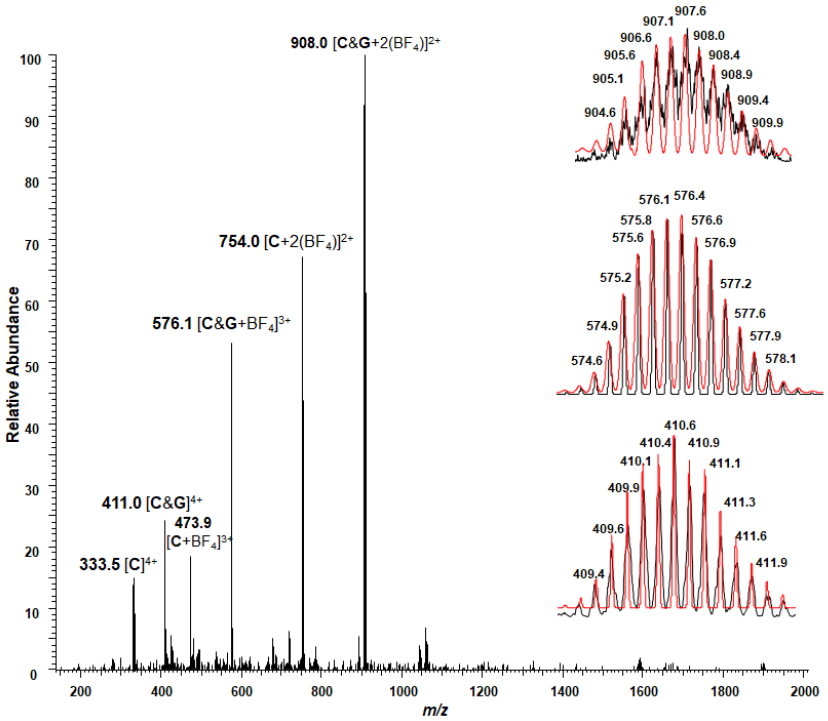

Figure S28. ESI-MS spectrum of $[Pd_2(\mathbf{2})_4\mathbf{G}]^{4+}$ (**G@C**) in DCM.

7. Binding Constant Measurements

7.1 Binding constants determined by UV-vis titration

The UV-vis titration technique was used to determine the binding constants of complexes. The full data of a selected wavelength region was analyzed using SPECFIT/32 global analysis system (Spectrum Software Associates, Marlborough, MA).

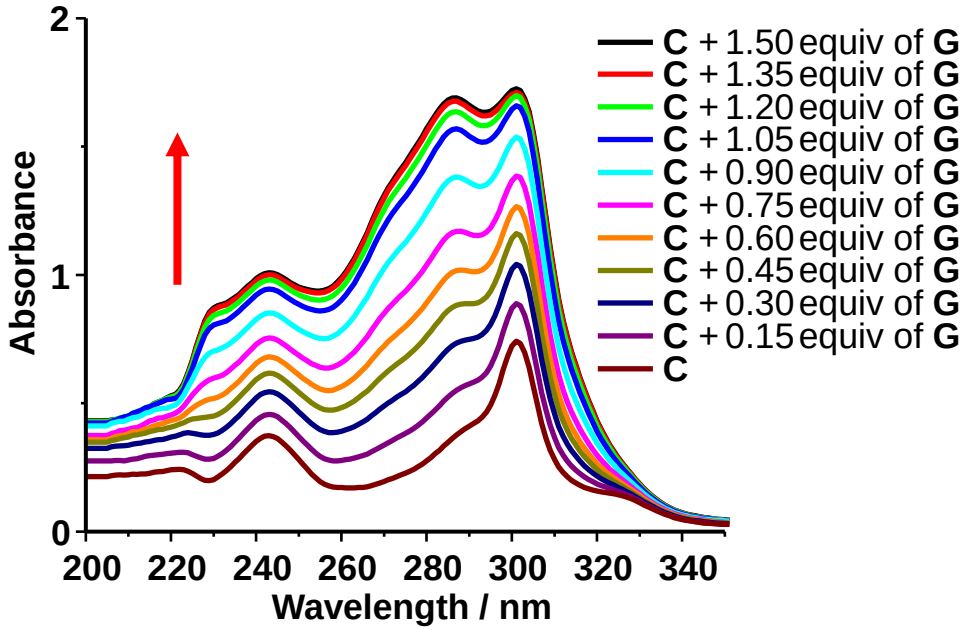

Figure S29. a) Stock solutions were prepared for **C** = $[Pd_2(\mathbf{2})_4]^{4+}$ (3.12×10^{-4} M) and guest pentacenedione (**G**) (3.12×10^{-4} M) in CH_2Cl_2. A UV-vis titration was performed between **C** (1.56×10^{-6} M) in CH_2Cl_2 (2.00 mL = volume after addition of 1 equiv of **C**) and **G** (3.12×10^{-4} M, 15.0 µL) in CH_2Cl_2 at 298 K to afford the complex **G@**$[Pd_2(\mathbf{2})_4]^{4+}$ = (**G@C**). The wavelength region 200 - 350 nm was analyzed. Result in CH_2Cl_2: log K = 8.02 ± 0.35. b) Stock solutions were prepared for **C** = $[Pd_2(\mathbf{2})_4]^{4+}$ (3.12×10^{-4} M) and guest pentacenedione (**G**) (3.12×10^{-4} M) in CH_2Cl_2:CH_3CN = 4:1. A UV-vis titration was performed between **C** (1.56×10^{-6} M) in CH_2Cl_2:CH_3CN = 4:1 (2.00 mL = volume after addition of 1 equiv of **C**) and **G** (3.12×10^{-4} M, 15.0 µL) in CH_2Cl_2:CH_3CN = 4:1 at 298 K to afford the complex **G@**$[Pd_2(\mathbf{2})_4]^{4+}$ = (**G@C**). The wavelength region 200-350 nm was analyzed. Result in CH_2Cl_2:CH_3CN = 4:1: log K = 7.91 ± 0.29.

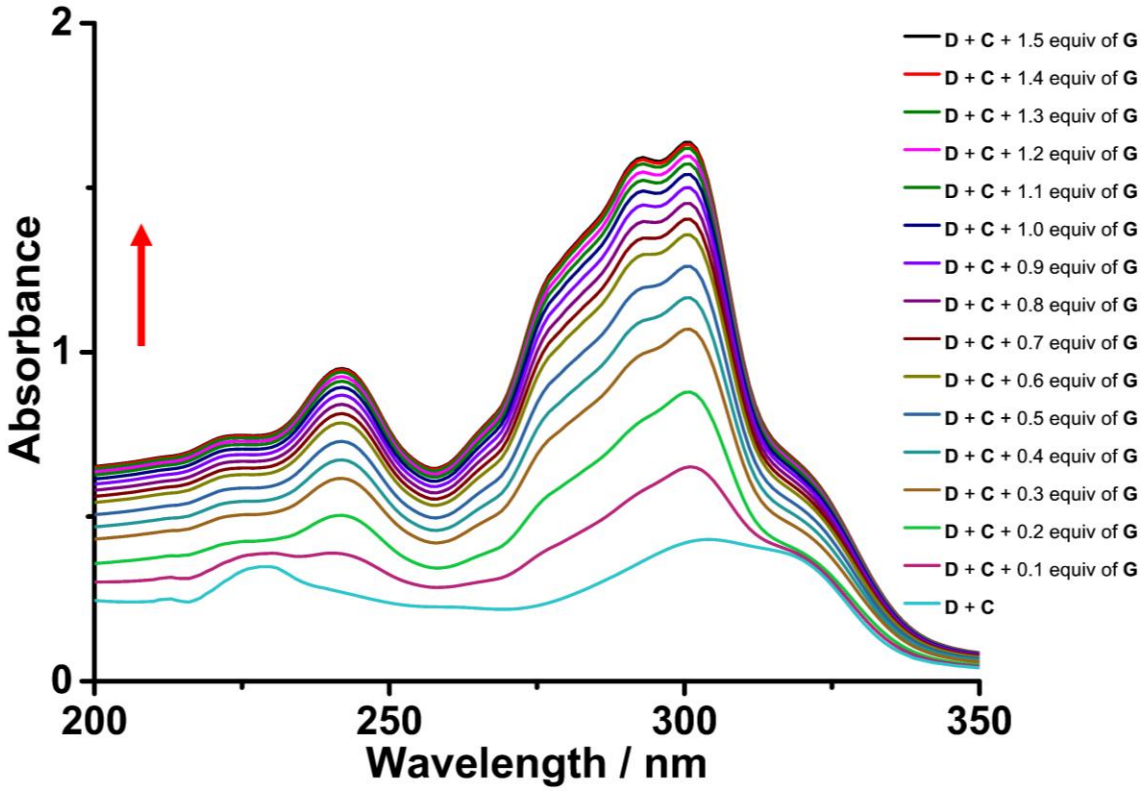

Figure S30. Initially, stock solutions were prepared for **C** = $[Pd_2(\mathbf{2})_4]^{4+}$ (3.12×10^{-4} M), **D** = $[Cu_3(\mathbf{1})]^{3+}$ (3.12×10^{-4} M) and pentacenedione (**G**) (3.12×10^{-4} M) in CH_2Cl_2:CH_3CN = 4:1. The UV-vis study was performed by titrating a mixture of **C** (1.56×10^{-6} M) and **D** (6.24×10^{-6} M) in CH_2Cl_2:CH_3CN = 4:1 (2.00 mL = volume) with **G** (3.12×10^{-4} M, 15.0 µL) in CH_2Cl_2:CH_3CN = 4:1 at 298 K to afford the complex $[Cu_3(\mathbf{1})]^{3+}$ + **G@**$[Pd_2(\mathbf{2})_4]^{4+}$ = **D** + (**G@C**). The wavelength region 200-350 nm was analyzed. Result in CH_2Cl_2:CH_3CN = 4:1: log K = 7.84 ± 0.18.

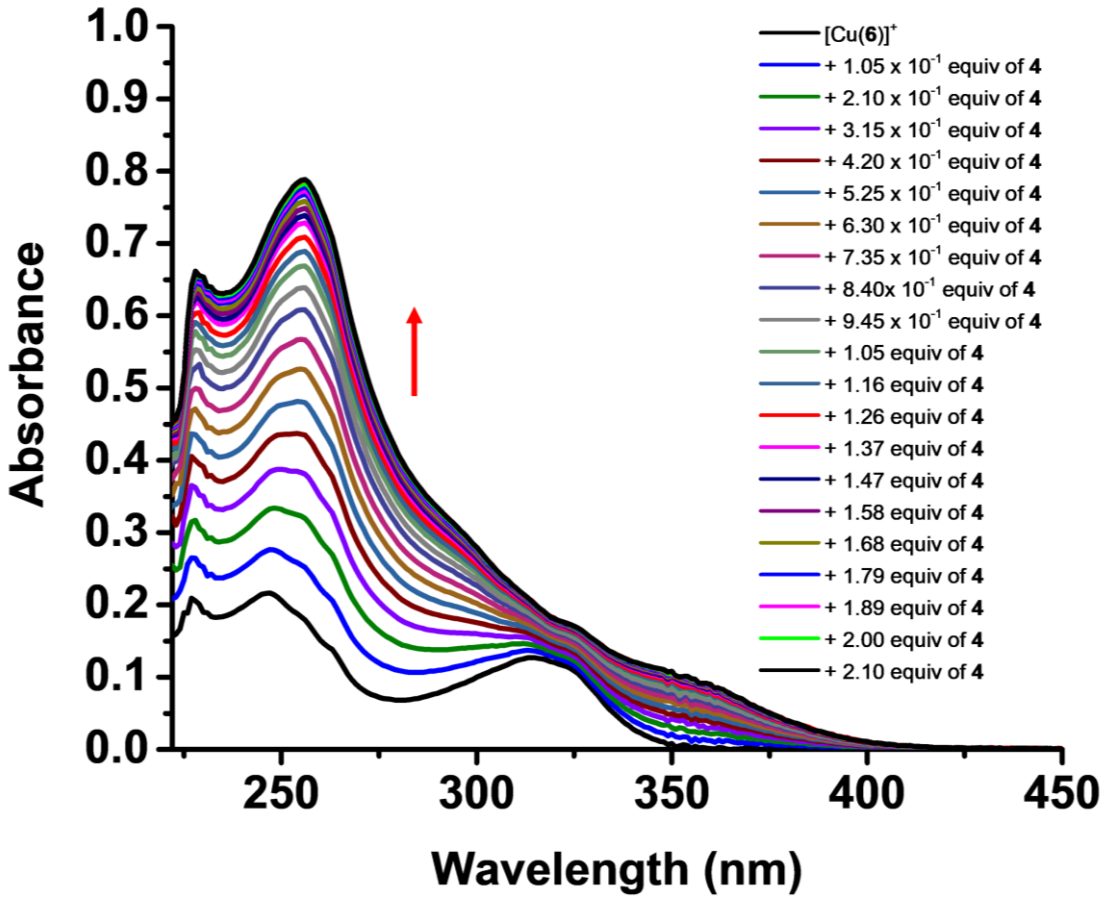

Figure S31. Stock solutions were prepared for $[Cu(\mathbf{6})]^+$ (2.44×10^{-4} M) and **4** (2.58×10^{-4} M) in CH_2Cl_2. A UV-vis titration was performed between $[Cu(\mathbf{6})]^+$ (1.22×10^{-6} M) in CH_2Cl_2 (2.00 mL = volume after addition of 1 equiv of $[Cu(\mathbf{6})]^+$) and **4** (2.58×10^{-4} M, 20.0 µL) in CH_2Cl_2 at 298 K to afford the complex $[Cu(\mathbf{6})(\mathbf{4})]^+$. The wavelength region 220 - 450 nm was analyzed. Result in CH_2Cl_2 log $K = 1.28 \pm 0.27$.

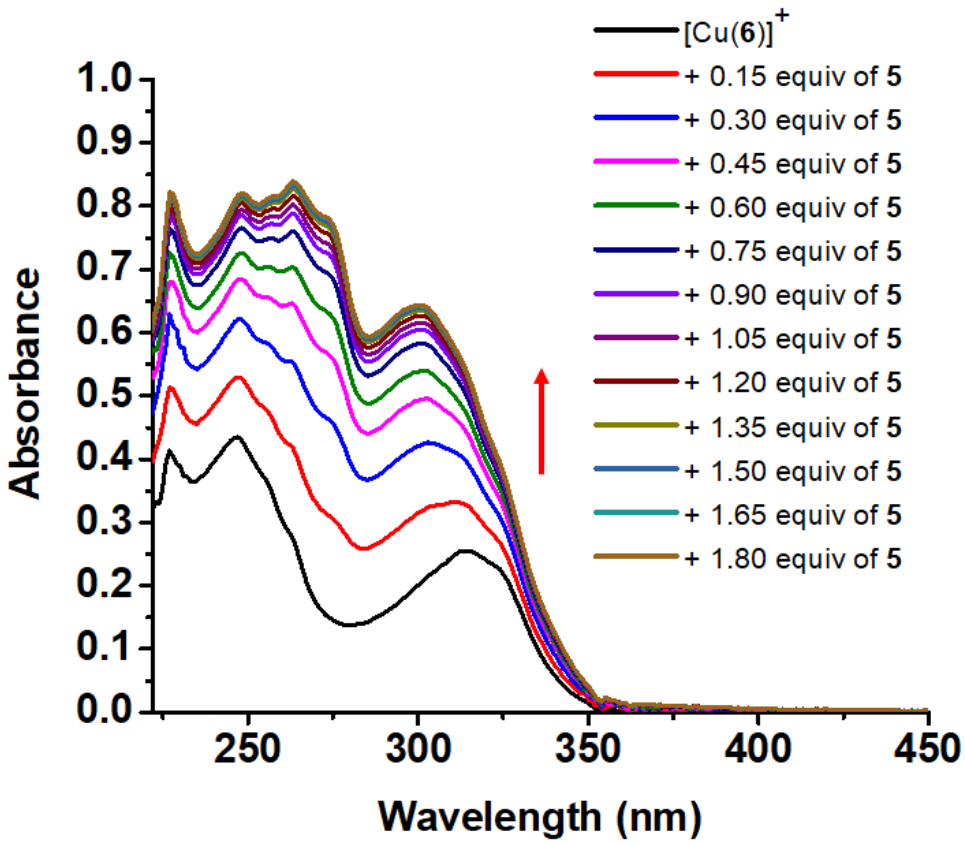

Figure S32. Stock solutions were prepared for $[Cu(\mathbf{6})]^+$ (2.44×10^{-4} M) and **5** (2.61×10^{-4} M) in CH_2Cl_2. A UV-vis titration was performed between $[Cu(\mathbf{6})]^+$ (1.22×10^{-6} M) in CH_2Cl_2 (2.00 mL = volume after addition of 1 equiv of $[Cu(\mathbf{6})]^+$) and **5** (2.61×10^{-4} M, 16.8 µL) in CH_2Cl_2 at 298 K to afford the complex $[Cu(\mathbf{6})(\mathbf{5})]^+$. The wavelength region 220 - 450 nm was analyzed. Result in CH_2Cl_2: log K = 1.91 ± 0.16.

7.2 Binding constants determined by ^{1}H NMR titration

To determine the binding constants between [Cu(**6**)]$^+$ and **4** as well as between [Cu(**6**)]$^+$ and **5** also the NMR titration method was used. An 3.38 mM solution of [Cu(**6**)]$^+$ was prepared in CD_2Cl_2 in an NMR tube. In other vessels, stock solutions of **4** (*c* = 121 mM) and **5** (*c* = 169 mM) were prepared in the same solvent. Small aliquots of solutions **4** and **5** were added. After each addition, the ^{1}H NMR was recorded and the peak at 6.95 ppm was monitored for data analysis. The binding constant was determined using a nonlinear curve-fitting applying the following equation:[5]

Y=Y0+DY*((K*(P+x)+1)–SQRT(((K*(P+x)+1)^2)–4*K*K*P*x))/(2*K*P)

Y = Measured Chemical shift; Y0 = Chemical shift of empty host solution; DY = Maximal change in chemical shift: the difference in chemical shift of a fully occupied host and an empty host; K = Binding constant; P = Total host concentration; x = Total guest concentration.

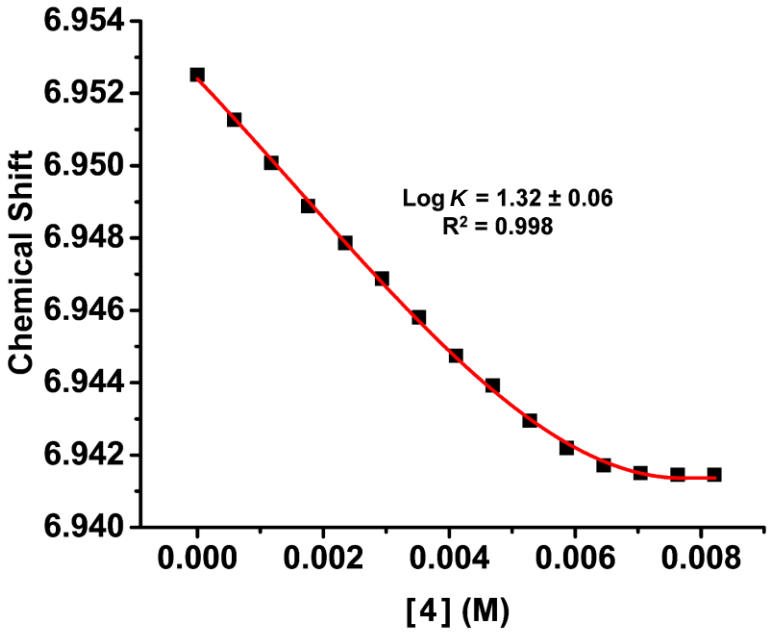

Figure S33. Curve-fitting for determination of binding constant between [Cu(**6**)]$^+$ and **4**. Result in CH_2Cl_2 log *K* = 1.32 ± 0.06.

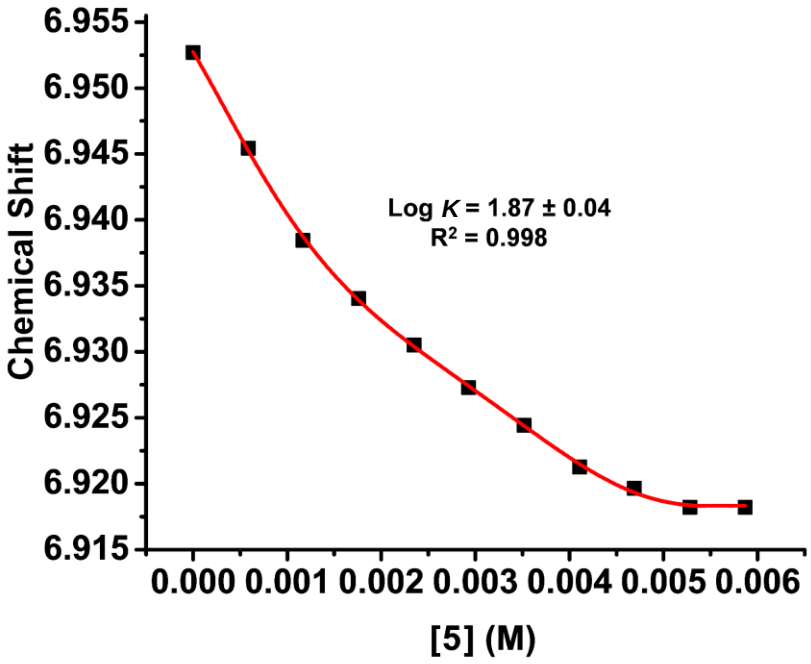

Figure S34. Curve-fitting for determination of binding constant between $[Cu(\mathbf{6})]^+$ and **5**. Result in CH_2Cl_2 log K = 1.87 ± 0.04.

8. Species Distribution Experiments

a) Speciation analysis of product **5** in relation to [Cu(**6**)]$^+$.

The species distribution was calculated using the Hyperquad software HySS2009® version applying log K = 1.91 ± 0.16 as the binding constant between [Cu(**6**)]$^+$ and **5** (0 → 1.22 × 10^{-4} M) at 298 K in CH_2Cl_2.

From the speciation distribution curve, we derive that 42% of complex [Cu(**6**)(**5**)]$^+$ is formed (at 1.22 × 10^{-6} M), thus leaving 58% of ligand **5** unbound. Reciprocally, it means that 58% of copper(I) ions are exposed to catalyze the aza Hopf cyclization of **4** to **5**.

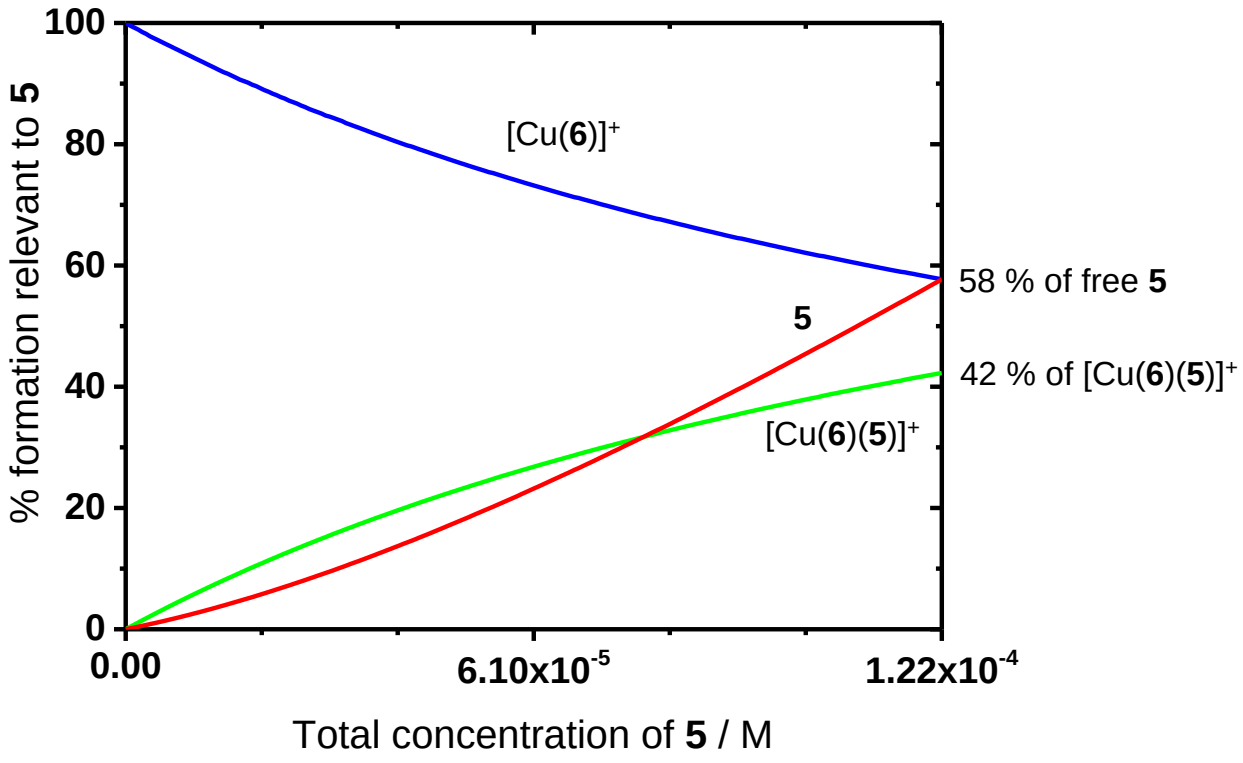

Figure S35. Calculated species distribution between [Cu(**6**)]$^+$ (1.22 × 10^{-6} M) with **5** (0 → 1.22 × 10^{-4} M) at 298 K in CH_2Cl_2 using log K = 1.91 ± 0.16.

b) Percentage of **5** liberated by slider-on-deck assembly.

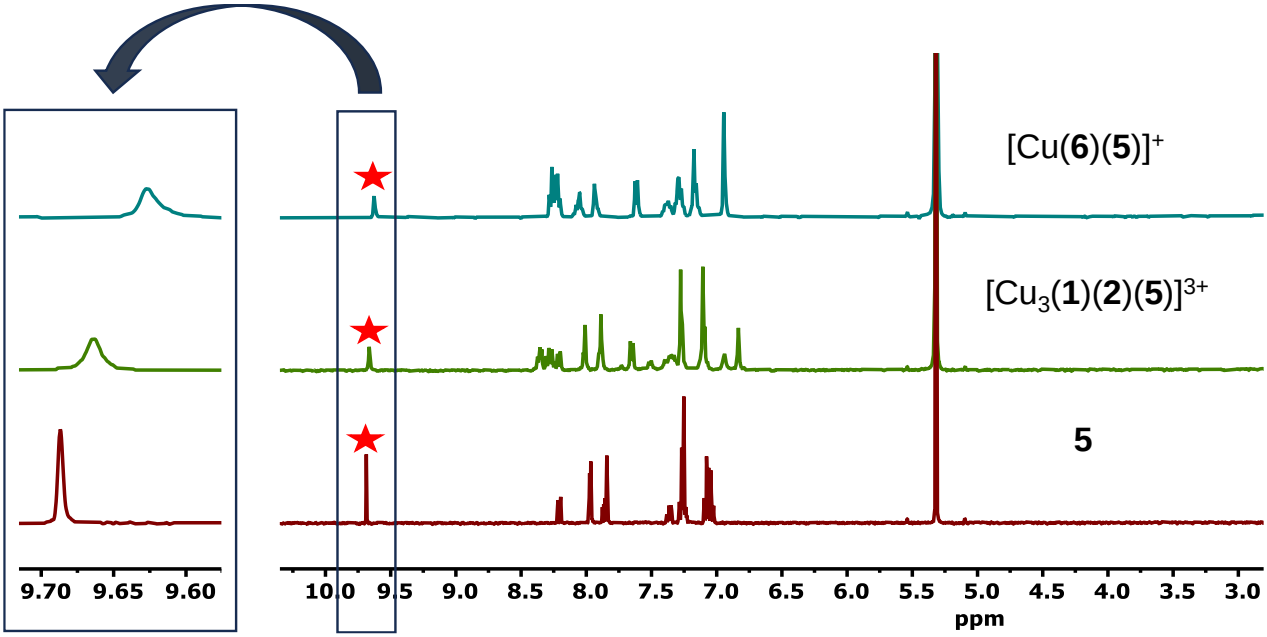

Figure S36. Partial ^{1}H NMR spectra (CD_2Cl_2:CD_3CN = 4:1, 400 MHz, 298 K) of product **5** (bottom), complex $[Cu_3(\mathbf{1})(\mathbf{2})(\mathbf{5})]^{3+}$ = **DS•5** (middle) and complex $[Cu(\mathbf{6})(\mathbf{5})]^{+}$ (up). The chemical shift of proton x'-H of **5** (see red asterisk) reveals that **5** is liberated into solution in $[Cu_3(\mathbf{1})(\mathbf{2})(\mathbf{5})]^{3+}$ due to the motion of biped **2**. This conclusion is supported by its chemical shift approaching that of free **5**.

Table S1. NMR shift and amount of **5** liberated from $[Cu_3(\mathbf{1})(\mathbf{2})(\mathbf{5})]^{3+}$ and $[Cu(\mathbf{6})(\mathbf{5})]^{+}$ at c = 3.38 mM.

Assemblies/ Compounds	δ / ppm[a]	**5** / %[b]
5	9.68	100
$[Cu_3(\mathbf{1})(\mathbf{2})(\mathbf{5})]^{3+}$	9.66	83
$[Cu(\mathbf{6})(\mathbf{5})]^{+}$	9.63	58

[a] Chemical shift of proton x'-H of **5** (CD_2Cl_2:CD_3CN = 4:1, 400 MHz, 298 K) in free **5** (top) and in various dynamic complexes. [b] Percentage of **5** liberated from the different complexes.

A prerequisite of the current analysis is that the exchange of **5** in free form and in $[Cu_3(\mathbf{1})(\mathbf{2})(\mathbf{5})]^{3+}$ or $[Cu(\mathbf{6})(\mathbf{5})]^{+}$ is fast on the NMR time scale providing an averaged shift.

The speciation analysis (SI, Figure S35) showed that 58% of **5** is liberated into solution from $[Cu(\mathbf{6})(\mathbf{5})]^{+}$ at the concentration $c = 1.22 \times 10^{-6}$ M as used in the UV-vis experiments. By means of the known chemical shifts of free **5** (δ = 9.68 ppm) and that (δ = 9.63 ppm) representing the

equilibrium of [Cu(**6**)]$^{+}$ + **5** ⇆ [Cu(**6**)(**5**)]$^{+}$ = 58 : 42 one can now derive the amount of **5** that is liberated from the assembly [Cu_3(**1**)(**2**)(**5**)]$^{3+}$ by its shift δ = 9.66 ppm as follows:

$\Delta\delta$ = chemical shift difference of product **5** (x'-H) between free (100%) and 58% unbound state in [Cu(**6**)(**5**)]$^{+}$, 9.68 - 9.63 = 0.05 ppm.

On the other hand, $\Delta\delta$1 is chemical shift difference of product **5** (x'-H) in the free and the bound state in [Cu_3(**1**)(**2**)(**5**)]$^{3+}$.

[Cu_3(**1**)(**2**)(**5**)]$^{3+}$ binds **5** in a yield = (100%-58%) x ($\Delta\delta1/\Delta\delta$) = [42% x (0.02/0.05)] = 17%. Therefore 83% of **5** is liberated from [Cu_3(**1**)(**2**)(**5**)]$^{3+}$.

9. Coordination Kinetics Studies

As the reaction order of the kinetic processes involved in the interconversion of both NetStates is unknown and follows an intricate mechanism, we decided to determine the approximate half-time of the reactions by using curve-fitting to the following simplified rate law:[6]

$$y = A1*\exp(-x/t1) + y0$$

We used the decrease in the absorbance intensity at the absorption maximum of the NetState-I (**DS + G**) (λ_{max} = 301 nm) as a function of time to derive the half-life (τ) of Pd(II)-coordination to **2**.

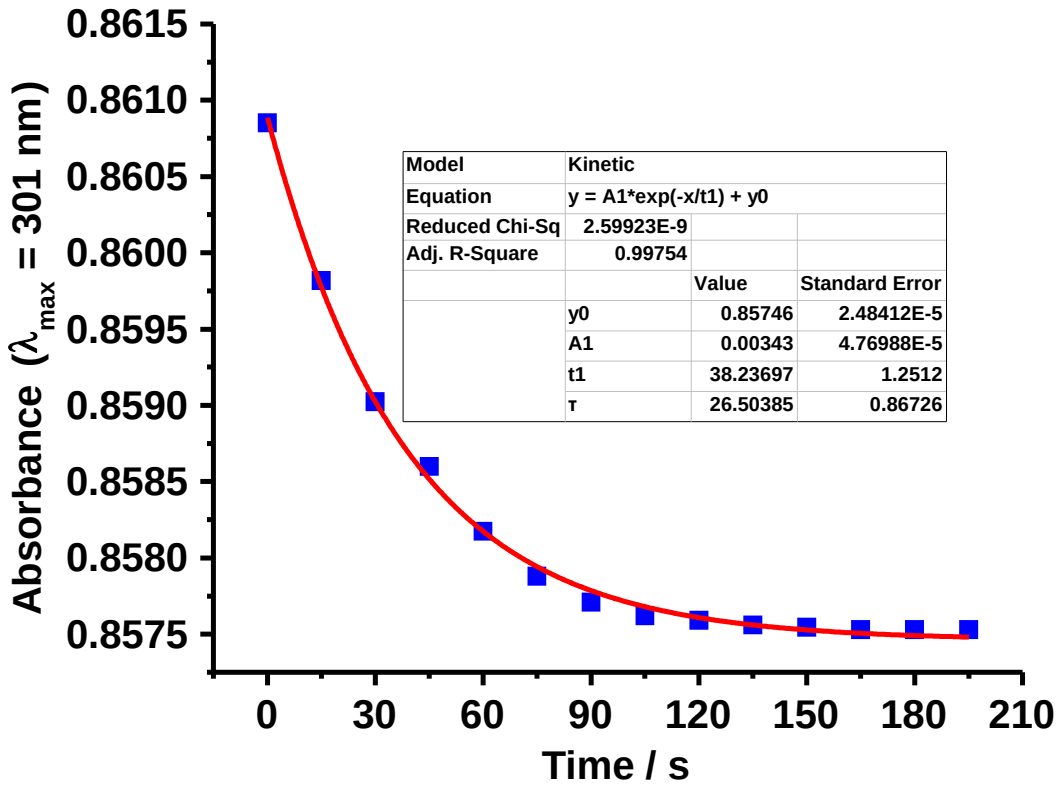

Figure S37. The kinetics of Pd(II) (2.44×10^{-4} M, in CD_2Cl_2:CD_3CN = 4:1) reacting with Netstate-I (**DS + G**) (1.22×10^{-6} M, 2.00 mL of CD_2Cl_2:CD_3CN (4:1) = total volume after addition of 1 equiv of $[Pd(CH_3CN)_4](BF_4)_2$) in CD_2Cl_2:CD_3CN = 4:1 at 298 K was followed by absorption spectroscopy at λ_{max} = 301 nm as a function of time. The Pd(II)-coordination half-life was determined to be 26.50 ± 0.87 s based on three consecutive measurements.

We used the increase in the absorbance intensity at the absorption maximum of the NetState-II (**D + G@C+ G**) (λ_{max} = 302 nm) as a function of time to derive the half-life (τ) of Pd(II)-coordination to DMAP.

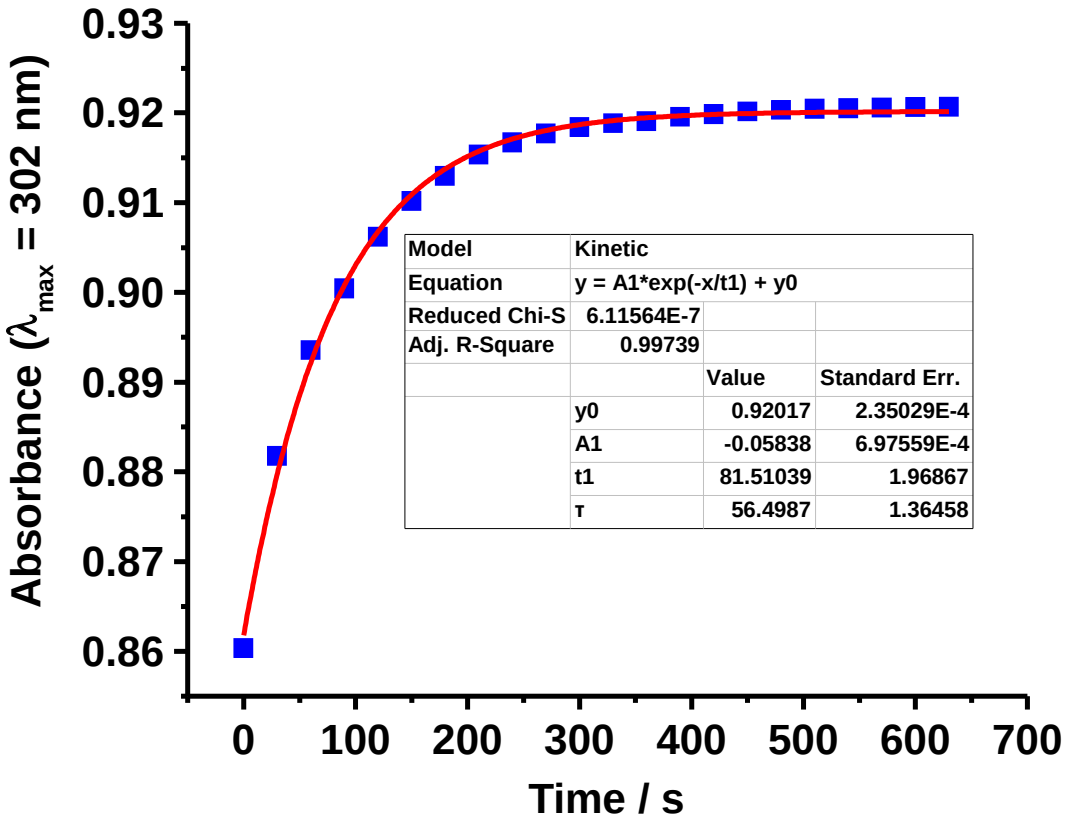

Figure S38. The kinetics of DMAP (2.44×10^{-4} M, in CD_2Cl_2:CD_3CN (4:1)) reacting with NetState-II (**D + G@C+ G**) (1.22×10^{-6} M, 2.00 mL of CD_2Cl_2:CD_3CN (4:1) = total volume after addition of 4 equiv of DMAP respect to Pd(II)) in CD_2Cl_2:CD_3CN (4:1) at 298K was followed by absorption spectroscopy at λ_{max} = 302 nm as a function of time. The Pd(II)-coordination half-live was determined to be 56.50 ± 1.36 s based on three consecutive measurements.

10. References

1. P. Liao, B. W. Langloss, A. M. Johnson, E. R. Knudsen, F. S. Tham, R. R. Juliana and R. J. Hooley, *Chem. Commun.*, 2010, **46**, 4932−4934. doi: 10.1039/c0cc00234h.

2. I. Paul, N. Mittal, S. De, M. Bolte and M. Schmittel, *J. Am. Chem. Soc.*, 2019, **141**, 5139−5143. doi: 10.1021/jacs.9b01182.

3. M. Schmittel, A. Ganz, W. A. Schenk and M. Hagel, *Z. Naturforsch. B.*, 1999, **54b**, 559−556.

4. Y.-F. Li, A. Ghosh, P. K. Biswas, S. Saha and M. Schmittel, *Chemistry*., 2021, **3**, 116–125. doi: 10.3390/chemistry3010009.

5. Y. R. Hristova, M. M. J. Smulders, J. K. Clegg, B. Breiner and J. R. Nitschke, *Chem. Sci*., 2011, **2**, 638−641. doi: 10.1039/c0sc00495b.

6. H. Fu, S. Pramanik and I. Aprahamian, *J. Am. Chem. Soc.*, 2023, **145**, 19554−19560. doi: 10.1021/jacs.3c02855.